Dual $\alpha_v\beta_6$ and $\alpha_v\beta_1$ Inhibition Over 12 Weeks Reduces Active Type 1 Collagen Deposition in Individuals with Idiopathic Pulmonary Fibrosis: A Phase 2, Double-Blind, Placebo-controlled Clinical Trial

Sydney B. Montesi,[1,2] Gregory P. Cosgrove,[3] Scott M. Turner,[4] Iris Y. Zhou,[2,5,6] Nikos Efthimiou,[2,5] Antonia Susnjar,[1,2] Ciprian Catana,[2,5,6] Caroline Fromson,[1] Annie Clark,[3] Martin Decaris,[3] Chris N. Barnes,[3] Éric A. Lefebvre,[3] Peter Caravan[2,5,6]

[1]Divison of Pulmonary and Critical Care Medicine, Massachusetts General Hospital, Boston, MA, USA; [2]Harvard Medical School, Boston, MA, USA; [3]Pliant Therapeutics, Inc., South San Francisco, CA, USA; [4]Former employee of Pliant Therapeutics, Inc., South San Francisco, CA, USA; [5]Athinoula A. Martinos Center for Biomedical Imaging, Department of Radiology, Massachusetts General Hospital, Charlestown, MA, USA; [6]Institute for Innovation in Imaging, Department of Radiology, Massachusetts General Hospital, Boston, MA, USA

Corresponding author:

Sydney B. Montesi

Massachusetts General Hospital

Division of Pulmonary and Critical Care Medicine

55 Fruit St

Boston, MA 02114

sbmontesi@mgb.org

AJRCCM Articles in Press. Published March 28, 2025 as 10.1164/rccm.202410-1934OC

Author contributions

All authors contributed to, reviewed, and approved the final draft of the paper. All authors had full access to all the data in the study and had final responsibility for the decision to submit for publication.

Concept and design: SBM, GPC, MD, ÉAL, and PC

Reconstruction of positron emission tomography data and quality control of positron emission tomography images: NE

Acquisition, analysis, or interpretation of data: SBM, GPC, IYZ, NE, AS, CC, CF, AC, MD, CNB, ÉAL, and PC.

Drafting of manuscript: all authors

Critical revision of the manuscript for important interllectual content: all authors

Statistical analysis: CNB

Funding

This study was sponsored by Pliant Therapeutics, Inc. Editorial assistance was provided by Samantha O'Dwyer, PhD, CMPP, of Nucleus Global and was funded by Pliant Therapeutics, Inc. Development of the imaging methodology employed and the radiochemistry equipment used in this study was supported by National Institutes of

AJRCCM Articles in Press. Published March 28, 2025 as 10.1164/rccm.202410-1934OC

Health awards (R01HL153606, K25HL148837, K23HL150331, S10OD028499, and S10OD032138)

Short title (50 characters maximum, including spaces; current: 42)**:** Bexotegrast Reduces Type 1 Collagen in IPF

Journal descriptor number: 9.23 Interstitial Lung Disease

Word count: 3500 maximum; current: **4009**

Figures and tables: no limit; current: 2 tables, 6 figures

Supplementary tables and figures: no limit; current: 2 figures

References: 50 maximum; current: 52

At a Glance Commentary

Scientific Knowledge on the Subject

IPF is characterized by excessive type 1 collagen deposition in the lungs via elevated transforming growth factor-beta (TGF-β) signaling. ^{68}Ga-CBP8 is a positron emission tomography (PET) probe that binds to type 1 collagen and has demonstrated increased uptake in the lungs of patients with IPF compared with healthy patients. Bexotegrast (PLN-74809) is an oral, once-daily, investigational drug that blocks the activation of TGF-β through the inhibition of $\alpha_v\beta_6$ and $\alpha_v\beta_1$ integrins.

AJRCCM Articles in Press. Published March 28, 2025 as 10.1164/rccm.202410-1934OC

What this study adds to the field

This PET imaging study suggests that changes in pulmonary type 1 collagen deposition can be monitored longitudinally in patients with IPF using ^{68}Ga-CBP8, and that bexotegrast demonstrated antifibrotic effects after 12 weeks of treatment. Similar changes in lung dynamic contrast-enhanced magnetic resonance imaging parameters were also observed. Improvements in forced vital capacity and cough severity occurred alongside the observed reductions in type 1 collagen, suggesting the potential of bexotegrast for disease modification.

Artificial Intelligence Disclaimer: No artificial intelligence tools were used in writing this manuscript.

This article has an online data supplement, which is accessible at the Supplements tab.

AJRCCM Articles in Press. Published March 28, 2025 as 10.1164/rccm.202410-1934OC

ABSTRACT

Rationale: Idiopathic pulmonary fibrosis (IPF) is characterized by excessive deposition of type 1 collagen. ^{68}Ga-CBP8, a type 1 collagen positron emission tomography (PET) probe, measures collagen accumulation and shows higher collagen deposition in patients with IPF. Bexotegrast (PLN-74809) is an oral, once-daily, dual-selective inhibitor of $\alpha_v\beta_6$ and $\alpha_v\beta_1$ integrins under late-stage evaluation for treatment of IPF.

Objectives: Evaluate changes in type 1 collagen in the lungs of participants with IPF following treatment with bexotegrast.

Methods: In this Phase 2 (NCT05621252), single-center, double-blind, placebo-controlled study, adults with IPF received bexotegrast 160mg or placebo for 12 weeks. Primary endpoint was the change in whole-lung standardized uptake value (SUV) of ^{68}Ga-CBP8 PET. Changes in lung dynamic contrast-enhanced magnetic resonance imaging (DCE-MRI) parameters, forced vital capacity (FVC), cough severity, and biomarkers of collagen synthesis and progressive disease were also assessed.

Measurements and Main Results: Of 10 participants, 7 received bexotegrast and 3 placebo. At Week 12, mean change from baseline in top quartile of ^{68}Ga-CBP8 whole-lung SUV was −1.2% with bexotegrast vs 6.6% with placebo; greatest mean changes were observed in subpleural lung regions in both groups (bexotegrast, −3.7%; placebo, 10.3%). DCE-MRI demonstrated numerically increased peak enhancement and faster contrast washout rate in bexotegrast-treated participants, suggesting improvements in lung microvasculature and decreased extravascular extracellular volume. Bexotegrast

AJRCCM Articles in Press. Published March 28, 2025 as 10.1164/rccm.202410-1934OC

treatment resulted in numerical improvements in FVC, cough severity, and biomarker levels.

Conclusions: The reduced uptake of ^{68}Ga-CBP8 in the lungs of participants with IPF indicates an antifibrotic effect of bexotegrast, suggesting the potential for favorable lung remodeling.

Trial registration number: NCT05621252

Keywords (3-5 max): IPF, PET imaging, bexotegrast, collagen type 1, fibrotic disease

Primary source of funding: Pliant Therapeutics, Inc.

Abstract word count: 250 words max; **current: 250**

AJRCCM Articles in Press. Published March 28, 2025 as 10.1164/rccm.202410-1934OC

INTRODUCTION

Idiopathic pulmonary fibrosis (IPF) is a chronic, progressive interstitial lung disease of unknown cause that is ultimately fatal(1, 2). IPF is characterized by a maladaptive response to lung injury that results in excessive type 1 collagen deposition and replacement of healthy tissue with collagen-rich scar tissue(3-5). Ongoing collagen deposition and crosslinking result in increasing extracellular matrix thickness and contribute to the distinctive expansive pulmonary fibrosis of IPF(6, 7). Progressive disease results in lung architectural distortion, worsening cough and dyspnea, and loss of lung function(2, 3). IPF is a heterogenous disease. Disease progression is highly variable and is not readily associated with characteristics such as age, sex, and baseline forced vital capacity (FVC)(8-10). Therapeutic options for patients with IPF are limited. Current approved treatments for IPF include pirfenidone and nintedanib, which slow disease progression but do not consistently improve symptom burden, lung function, or quality of life(11, 12).

Elevated transforming growth factor-beta (TGF-β) signaling is a hallmark of IPF; TGF-β activation mediates fibrosis through fibroblast activation and proliferation, which drive collagen synthesis and result in tissue stiffness(13-16). α_v integrins such as $\alpha_v\beta_6$ integrin, expressed by lung epithelial cells, and $\alpha_v\beta_1$ integrin, expressed by lung fibroblasts, are overexpressed in the lungs of patients with IPF and can convert latent TGF-β into its active form(17-19). As TGF-β is involved in multiple biological functions, systemic inhibition carries safety risks(14, 20). Specific targeting of $\alpha_v\beta_6$ and $\alpha_v\beta_1$ integrins may therefore provide a localized, safer approach to TGF-β inhibition in the fibrotic lung.

AJRCCM Articles in Press. Published March 28, 2025 as 10.1164/rccm.202410-1934OC

Bexotegrast (PLN-74809) is an oral, once-daily, dual-selective inhibitor of $\alpha_v\beta_6$ and $\alpha_v\beta_1$ integrins and is in late-stage development for the treatment of IPF (BEACON-IPF; NCT06097260). Studies in animal models and precision-cut lung slices from explanted tissue of patients with IPF suggest that bexotegrast can reduce collagen deposition and collagen gene expression by as much as 50%(19). In a Phase 2 study of participants with IPF (INTEGRIS-IPF; NCT04396756), treatment with bexotegrast for ≤40 weeks demonstrated a favorable safety profile with suggested improved lung function based on FVC and antifibrotic effects based on quantitative lung fibrosis imaging and circulating biomarkers(21). After 12 weeks, treatment with bexotegrast 160 or 320 mg improved FVC compared with placebo in a participant population in which ≈80% were receiving pirfenidone or nintedanib background therapy(21). Quantitative assessment of lung imaging using high-resolution computed tomography (HRCT) demonstrated no or limited fibrotic progression in participants receiving bexotegrast 160 or 320 mg compared with progression observed with placebo(21). However, current imaging approaches only visualize the result of collagen deposition (eg, reticular opacities and honeycombing) and do not provide clear insight into ongoing, new collagen deposition in the lung.

^{68}Ga-CBP8 is a positron emission tomography (PET) probe that binds to type I collagen in fibrotic lung tissue(22-24). In mouse models of pulmonary fibrosis, ^{68}Ga-CBP8 correlated with levels of fibrosis following injury and revealed a response to antifibrotic therapy with an antibody targeting $\alpha_v\beta_6$ integrin(23, 24). In a noninterventional study, ^{68}Ga-CBP8 showed higher collagen levels in patients with IPF compared with healthy individuals, particularly in the subpleural region of the lung where

AJRCCM Articles in Press. Published March 28, 2025 as 10.1164/rccm.202410-1934OC

the disease is most prominent(22). ^{68}Ga-CBP8 PET was assessed using standardized uptake values (SUVs), which measure the uptake or signal intensity of the probe in tissue; a higher SUV reflects a higher concentration of the probe and, thus, more collagen. ^{68}Ga-CBP8 PET showed increased uptake in areas that appeared normal (prior to architectural distortion) on HRCT in patients with IPF, suggesting that it may be more sensitive than HRCT in detecting active or early fibrosis(22).

Dynamic contrast-enhanced magnetic resonance imaging (DCE-MRI) using an extracellular fluid, gadolinium-based contrast agent can provide functional and anatomical information on the lung. The percentage peak signal enhancement following contrast administration and the washout rate ($k_{washout}$) of contrast from the lung parenchyma can provide key information on microvascular function and extravascular extracellular volume, respectively(25-27). In non-interventional studies in patients with IPF, lower peak enhancement and slower $k_{washout}$ rates were observed compared with healthy volunteers(28). Slower $k_{washout}$ is likely due to one of several processes that expand the extravascular extracellular volume, including edema, inflammation, and fibrosis. Using ^{68}Ga-CBP8 PET combined with DCE-MRI allows for multimodal direct and indirect assessments of lung collagen and fibrosis in a single examination.

The primary objective of this study was to quantify changes in type 1 collagen in the lungs of participants with IPF following 12 weeks of treatment with bexotegrast 160 mg using ^{68}Ga-CBP8 PET combined with DCE-MRI. Safety, tolerability, efficacy, effect on cough, and biomarkers of collagen synthesis and disease progression were also assessed. A portion of these results have been previously published in the form of an abstract.(29)

AJRCCM Articles in Press. Published March 28, 2025 as 10.1164/rccm.202410-1934OC

METHODS

Study design

This Phase 2a, single-center, randomized, double-blind, placebo-controlled study (NCT05621252) was conducted at Massachusetts General Hospital, Boston, MA, USA. The treating physician, those acquiring the images, the image analysts and patients were all blinded in this study. Participants were randomized 2:1 to receive once-daily oral bexotegrast 160 mg or placebo for 12 weeks, with 2 weeks of follow-up (**Fig 1A**). A dose of 160 mg is expected to achieve the target 50% inhibitory concentration (≈500 ng/mL) for $\alpha_v\beta_6$ and $\alpha_v\beta_1$ integrin–mediated TGF-β activation for 24 hours(21). No dose modifications were permitted for bexotegrast. This study was conducted in accordance with the Declaration of Helsinki, the study protocol, and the International Council on Harmonization Good Clinical Practice regulations. The Mass General Brigham Institutional Review Board approved the study. All participants provided written informed consent.

Study population

The study enrolled participants aged ≥40 years with a diagnosis of IPF within 8 years prior to screening, according to the American Thoracic Society/European Respiratory Society/Japanese Respiratory Society/Latin American Thoracic Society 2018 Clinical Practice Guideline(30), with forced vital capacity percent predicted (FVCpp) of ≥45%, hemoglobin-adjusted diffusing capacity for carbon monoxide of ≥30%, and an estimated glomerular filtration rate of ≥50 mL/min. If IPF diagnosis was >3 years prior to

AJRCCM Articles in Press. Published March 28, 2025 as 10.1164/rccm.202410-1934OC

screening, the participant must have a decline in FVCpp ≥5% within the prior 24 months. Background therapy for IPF with pirfenidone or nintedanib was permitted but not mandated, provided these drugs had been given at a stable dose for ≥3 months prior to screening. Key exclusion criteria included receiving any non-approved agent intended to treat IPF, a forced expiratory volume during the first second (FEV_1)/FVC ratio of <0.7, and known or suspected acute IPF exacerbation within 6 months of screening.

Study objectives

The primary endpoint was the quantification of type 1 collagen in the lung, which was assessed using changes from baseline in ^{68}Ga-CBP8 PET SUV following 12 weeks of bexotegrast treatment. The key secondary endpoint was the safety and tolerability of bexotegrast. Key exploratory endpoints were the change from baseline in DCE-MRI contrast peak enhancement and washout rate, change from baseline in absolute FVC and FVCpp, change from baseline in cough severity, and plasma and serum biomarker analysis for type III collagen synthesis neoepitope (PRO-C3) and progressive fibrosing interstitial lung disease biomarker integrin beta-6 (ITGB6).

Procedures

Participants underwent a combined PET/MRI scan within 7 days prior to baseline (Day 1) and within 7 days prior to Week 12. Full details are in the supplemental methods.

Statistical analysis

AJRCCM Articles in Press. Published March 28, 2025 as 10.1164/rccm.202410-1934OC

Given the limited sample size, only descriptive statistics were planned for this study. No statistical comparison was planned. For PET, SUV summary metrics, including the mean (mean of all SUVs by voxel within a region), maximum (maximum SUV by voxel within a region), and top quartile SUV (mean of highest 25% SUVs by voxel within a region) change from baseline, were reported. The top quartile metric was selected as the primary endpoint to capture areas of most active disease within each region. For DCE-MRI, contrast peak enhancement, time to peak, and $k_{washout}$ change from baseline were reported. Incidence and severity of treatment-emergent adverse events (TEAEs) were summarized using count and proportion of participants. Absolute FVC and FVCpp change from baseline values are presented using least-squares means to adjust for differing baseline levels. The patient-reported outcome of cough severity as assessed on a 100-mm linear visual analog scale (VAS) from 0 mm (no cough) to 100 mm (most severe cough) was completed at screening, baseline, and Weeks 2, 3, 6, 12, and 14 and summarized as change from baseline.

Correlations between changes in top-quartile SUV, FVC, FVCpp, and biomarkers were described using the Spearman correlation coefficient. Frequency counts and percentages were used for categorical variables, and medians (IQRs), means, SDs, and SEs were used for continuous variables. Further details are in the online supplement.

RESULTS

Study participants

A total of 10 participants met the eligibility criteria. Participants were randomized to once-daily bexotegrast 160 mg (n=7) or placebo (n=3) (**Fig 1A**). All participants

AJRCCM Articles in Press. Published March 28, 2025 as 10.1164/rccm.202410-1934OC

completed 12 weeks of treatment (**Fig 1B**). Mean (SD) age (bexotegrast vs. placebo) was 69.1 (8.3) vs. 74.0 (2.0) years, 85.7% vs. 100% of participants were male, and 85.7% vs. 100% were White (**Table 1**). Eight participants (80.0%) received background therapy; 6 (60.0%) received nintedanib and 2 (20.0%) pirfenidone. The median (IQR) time since diagnosis was 50 (22.0-70.0) months and 9 (7.0-72.0) months in the bexotegrast and placebo groups, respectively. Baseline median (IQR) percent predicted FVC (FVCpp) was 66.0% (56.0%-92.0%) with bexotegrast and 58.0% (49.0%-69.0%) with placebo. The median (IQR) baseline cough severity in bexotegrast- and placebo-treated participants were 28.0 (5.0-66.0) mm and 19.0 (0-45.0) mm, respectively.

Lung collagen deposition

After 12 weeks of treatment, the numerical directionality favored a mean (SE) [%] decrease of −0.015 (0.038) [−1.2%] from baseline in the whole-lung top quartile of SUVs for bexotegrast 160 mg (**Fig 2A, 2B, 2C, and E1A**), indicating a reduction in total lung collagen. Four of 7 participants in the bexotegrast 160-mg group had a stable or reduced top quartile SUV change from baseline (**Fig 2B and 2C**), ranging from −15.6% to 0% (**Fig E1A**). Two participants demonstrated a 1.3% to 3.1% increase. Notably, 1 bexotegrast-treated participant had a numerically large increase from baseline (17.4%), which may have resulted from non-adherence to the study drug (65% study drug adherence with <80% compliance each month on study) and contracting COVID-19 in the first month of treatment.

The SUV changes at Week 12 were largest in the subpleural lung regions. Mean (SE) [%] change from baseline in the subpleural top quartile SUV in the bexotegrast

AJRCCM Articles in Press. Published March 28, 2025 as 10.1164/rccm.202410-1934OC

group was −0.051 (0.056) [−3.7%] (**Fig 3A and E1B**). Five of 7 participants had a reduced top quartile SUV, ranging from −19.6% to −4.0%; 1 participant demonstrated a small increase (1%), while the participant who was non-adherent to the study drug demonstrated a 19.0% increase. The reduction in SUVs in the subpleural regions was generally consistent across treated participants, with 5 of 7 showing decreases in the upper and middle regions and 4 of 7 showing decreases across all 3 subpleural regions (**Fig 3B**).

Conversely, the placebo group had numerical directionality that favored a mean (SE) [%] increase of 0.074 (0.068) [6.6%] from baseline in the top quartile SUV (**Fig 2B, 2C and E1A**) of the whole lung and 0.128 (0.079) [10.3%] (**Fig 3A and E1B**) in the subpleural whole lung. Two of 3 placebo-treated participants had increases in both the whole-lung and subpleural region top quartile SUVs (**Fig 2B, 2C,and Fig E1**). One placebo-treated participant had a slight reduction (−1%).

Changes in the central lung region in both treatment groups were less pronounced and less consistent than those in the subpleural region (**Fig 3A and 3B**). The mean (SE) [%] change from baseline in the central region was −0.003 (0.026) [−0.2%] and 0.020 (0.050) [2.0%] in the bexotegrast and placebo group, respectively (**Fig 3B and E1B**). Two participants in the bexotegrast group showed reductions in the central whole lung (−15.4% and −11.6%), and 5 showed increases (1.1%-8.2%) (**Fig E1B**). Two participants in the placebo group showed reductions in the central whole lung (−5.7% and −1.6%), and 1 showed increases (13.7%) (**Fig E1B**).

DCE-MRI showed changes in peak contrast enhancement and $k_{washout}$ in the whole lung over 12 weeks of treatment with bexotegrast. Absolute median (IQR) [%] change in

AJRCCM Articles in Press. Published March 28, 2025 as 10.1164/rccm.202410-1934OC

peak enhancement increased from baseline by 12.0% (−2.00%, 29.00%) [10.0%] (**Fig 4A**), consistent with increased pulmonary perfusion and/or decreased vascular permeability. The peak enhancement in 4 of 6 participants either remained stable or increased (**Fig 4A and 4B**), ranging from 6.0% to 53.0%. The bexotegrast-treated participant with study drug non-adherence and COVID-19 had a large decrease from baseline (−69.0%).

Participants in the bexotegrast group demonstrated an absolute median (IQR) [%] change from baseline in $k_{washout}$ of −1.06% (−1.50%, −0.72%) [31.7%] per minute (**Fig 4C**), indicating faster washout after treatment with bexotegrast and consistent with a reduction in the extravascular extracellular volume of the lung. Of the 7 participants, 5 had a faster rate compared with baseline (**Fig 4C and 4D**), while the participant with study drug non-adherence and COVID-19 had a slower rate (3.38% per minute) compared with baseline.

Similar to the pattern observed with SUVs where placebo showed more collagen deposition compared with baseline, the placebo group had an absolute median (IQR) [%] change from baseline in peak enhancement of −21.0% (−24.0%, −19.0%) [−16.1%], (**Fig 4A**). All 3 placebo-treated participants had decreased peak enhancement ranging from −24.0% to −19.0% (**Fig 4A and 4B**). Participants in the placebo group demonstrated an absolute median (IQR) [%] change from baseline in $k_{washout}$ of 0.07% (−0.69%, 1.63%) [0.8%] per minute (**Fig 4C**), indicating slower washout after placebo treatment and suggesting an increase in extravascular extracellular volume. Of the 3 participants, 2 had $k_{washout}$ values ranging from 0.07 to 1.63% per minute compared to baseline (ie, slower washout compared to baseline) (**Fig 4C and 4D**). Representative

AJRCCM Articles in Press. Published March 28, 2025 as 10.1164/rccm.202410-1934OC

DCE-MRI lung maps for peak enhancement and $k_{washout}$ at baseline and Week 12 from participants in the bexotegrast and placebo groups are shown in **Fig 4E** and demonstrate the heterogeneity in these parameters throughout the lung and how they change with treatment.

Exploratory endpoints

Treatment with bexotegrast resulted in numerically reduced FVC decline over 12 weeks, with the bexotegrast group maintaining a clear separation from the placebo group at all time points. At Week 12, the least-squares mean (SE) change from baseline in FVC was 14.5 (46.30) mL and −91.5 (73.98) mL in the bexotegrast and placebo groups, respectively (**Fig 5A**). The least-squares mean (SE) change from baseline in FVCpp was 1.4% (1.53%) and −2.6% (1.89%) in the bexotegrast and placebo groups, respectively (**Fig 5B**). Changes in top quartile SUV were moderately negatively correlated with changes in FVC and FVCpp: −0.57 and −0.63, respectively. Participants in the bexotegrast group reported decreased cough severity across all on-treatment time points compared with the placebo group (**Fig 5C**). Individual FVC and cough severity data are presented in **Fig E2**. Circulating-biomarker analysis revealed decreases in markers of collagen synthesis, represented by PRO-C3 (**Fig 6A** and **Fig E3**) and ITGB6 (**Fig 6B** and **Fig E3**), in the bexotegrast vs placebo group after 12 weeks of treatment.

Safety

AJRCCM Articles in Press. Published March 28, 2025 as 10.1164/rccm.202410-1934OC

Overall, bexotegrast demonstrated a favorable safety and tolerability profile over 12 weeks of treatment (**Table 2**). Six bexotegrast-treated participants (85.7%) and 1 placebo-treated participant (33.3%) reported ≥1 TEAE. The most frequently reported on-treatment TEAE in the bexotegrast group was diarrhea (3 participants, 42.9%). All events of diarrhea were considered mild; all participants in the bexotegrast group who had diarrhea were receiving concomitant nintedanib treatment. Most TEAEs were mild to moderate in severity. No serious AEs occurred in the study. One participant in the bexotegrast group receiving background therapy with nintedanib had asymptomatic Grade 3 TEAEs of increased amylase and increased lipase. One participant in the bexotegrast group had a TEAE of COVID-19 that led to an interruption of the study drug; this participant did not withdraw or terminate the study early. No deaths occurred during the study.

DISCUSSION

Collagen accumulation in the lungs of patients with fibrotic lung disease, particularly those with IPF, is the hallmark of disease progression. Current imaging modalities only detect pathological structural abnormalities resulting from aberrant collagen deposition. Changes in lung uptake of the type I collagen PET probe ^{68}Ga-CBP8 correlated with lung collagen content and may be a more sensitive measure of active disease and a tool to assess the early therapeutic effects of antifibrotic drugs(23, 31). The results from this study support the detection of less total lung collagen using ^{68}Ga-CBP8 PET imaging, after 12 weeks of bexotegrast 160 mg treatment, suggesting the potential of bexotegrast to substantially reduce the fibrotic accumulation process.

AJRCCM Articles in Press. Published March 28, 2025 as 10.1164/rccm.202410-1934OC

To our knowledge, this is the first interventional Phase 2 study to evaluate type 1 collagen deposition in the lungs of participants with IPF. Previous studies have demonstrated the use of molecular imaging for the characterization and localization of fibrosis-related processes(22, 23, 32, 33); however, these were either conducted in preclinical mouse models or in human participants who underwent imaging at a single time point. A unique aspect of this study was the ability to follow disease progression in participants over 12 weeks. In this study, collagen deposition increased from baseline in placebo-treated participants, consistent with increases in fibrotic reticular patterns seen in participants with IPF in other Phase 2 or 3 studies(21, 34, 35), whereas collagen deposition decreased from baseline in bexotegrast-treated participants. These results suggest that changes in pulmonary collagen deposition can be monitored longitudinally in patients with IPF using ^{68}Ga-CBP8 PET imaging and provide important information on early treatment effects.

IPF is a disease that predominately affects the subpleural lung regions(2). Prior use of ^{68}Ga-CBP8 PET in participants with IPF demonstrated that probe uptake was greatest in the subpleural regions(22). Our findings also corroborated this, as we saw that SUV levels in participants were numerically higher in all subpleural regions than in the central region. Additionally, the effect of bexotegrast appeared to be predominant in the subpleural regions, as the ^{68}Ga-CBP8 SUVs in bexotegrast-treated participants decreased in each subpleural region, whereas it increased in placebo-treated participants over 12 weeks. For this study we utilized mean of the top quartile of SUVs within each region of interest as our primary PET measurement. Presently, there are no established PET imaging measurements for use in lung studies. Current imaging

AJRCCM Articles in Press. Published March 28, 2025 as 10.1164/rccm.202410-1934OC

modalities (eg, computed tomography) only detect pathological structural abnormalities resulting from aberrant collagen deposition. Given the heterogeneity of the diseased lung in IPF, the use of top quartile SUV presents an opportunity to more accurately represent the probe uptake within regions with a greater extent of fibrosis thereby maximizing the ability to measure change over a short period of time.

The reduction of lung ^{68}Ga-CBP8 uptake with bexotegrast treatment provides evidence of the pharmacodynamic effect and potential efficacy of bexotegrast in participants with IPF and supports the role of non-invasive imaging of type 1 collagen as an important biomarker of disease activity. Bexotegrast blocks the activation of TGF-β by inhibiting $\alpha_v\beta_6$ and $\alpha_v\beta_1$ binding to latent TGF-β(19). The PET data from this study are consistent with preclinical findings suggesting that bexotegrast interrupts the fibrotic process by blocking TGF-β activation and subsequent type 1 collagen deposition. Our study supports the hypothesis that bexotegrast reduces collagen deposition in the lungs of participants with IPF and builds on previous evidence of bexotegrast's antifibrotic mechanism of action using quantitative lung imaging (21).

Changes in DCE-MRI measurements of contrast peak enhancement and washout rates after treatment with bexotegrast mirrored our PET imaging data. Patients with IPF have reduced lung peak enhancement(22), suggesting leakage of capillaries within the lung and worsening perfusion(36, 37). These data add to this body of knowledge. Participants treated with placebo had decreased peak enhancement over 12 weeks, suggesting that lung perfusion decreased over time, consistent with prior results(37). Additionally, the rate of contrast washout from the lungs has been shown to be slower in patients with IPF compared with healthy controls, reflecting the larger

AJRCCM Articles in Press. Published March 28, 2025 as 10.1164/rccm.202410-1934OC

amount of matrix accumulating in extravascular extracellular space and consistent with the replacement of lung cells by abnormal, collagen-rich extracellular matrix in IPF(28, 38). DCE-MRI methods are established in other organs such as the heart and liver for quantification of the extravascular volume as an indirect measurement of fibrosis(39, 40). An interesting observation from our study is that treatment with bexotegrast led to increased peak enhancement (improved perfusion and decreased microvascular permeability) and faster contrast washout rate (decreased extracellular extravascular volume). These findings, in combination with the PET data, suggest the potential for favorable lung remodeling resulting from decreased deposition of new collagen, and restoration of the homeostatic balance between collagen synthesis and degradation(41). Together, the multimodal data corroborate an antifibrotic mechanism of bexotegrast and support continued clinical development.

Consistent with other Phase 2 data in a larger patient population (n=120)(21), the exploratory efficacy and biomarker results provide evidence of a treatment effect of bexotegrast in participants with IPF. The results from this study were consistent with improvements in quantitative lung fibrosis and FVC, and further supported by reductions in known biomarkers of IPF progression(21). A separation in FVC between bexotegrast and placebo groups was observed as early as Week 4 and at all measured time points through Week 12. Additionally, participants treated with bexotegrast self-reported improved cough severity compared with those who received placebo at each on-treatment time point over 12 weeks of treatment. Once treatment ended, cough events returned, which may be an indicator of disease progression(42). While the pathogenesis of cough in IPF is poorly understood and no treatments are available(43), the

AJRCCM Articles in Press. Published March 28, 2025 as 10.1164/rccm.202410-1934OC

overexpression of TGF-β in airway epithelial cells in patients with chronic cough may be associated with a common pathobiology(43, 44). Therefore, these results suggest that TGF-β pathway inhibition by bexotegrast may play a role in decreasing cough in patients with IPF. By Week 12, improvements in cough in the bexotegrast-treated group were approaching clinical meaningfulness(45). PRO-C3 has been shown to be elevated in patients with IPF and is associated with progressive disease, and elevated ITGB6 plasma levels are associated with interstitial lung disease progression(46-48). At the end of the study, bexotegrast-treated participants showed decreases in the prognostic biomarkers PRO-C3 and ITGB6. These correlated functional and symptom changes, combined with evidence of reduced lung collagen and extracellular volume, suggest the potential of bexotegrast for disease modification.

Taken together, the efficacy and biomarker data presented in this study and the previous INTEGRIS-IPF study illustrate potential treatment effects. Late-stage evaluation of bexotegrast will further explore its efficacy and safety in participants with IPF (BEACON-IPF; NCT06097260).

This study should be interpreted in the context of some limitations, most notably the small sample size of the treatment sample. Due to the small size, disease characteristics were not completely balanced. Given only n=3 participants were in the placebo group, it is expected that there will be differences in percentages in categorical baseline characteristics (eg, sex, race, and background therapy) compared with the bexotegrast group (n=7); a single participant could change the percentage by 33%. Correspondingly, imbalances in continuous variables (eg, age, FVC, FVCpp) are expected given the heterogeneity in the IPF sample where a single participant could

AJRCCM Articles in Press. Published March 28, 2025 as 10.1164/rccm.202410-1934OC

change the mean or median value by a large margin. Previous subgroup analyses have found limited differences in treatment effect in baseline characteristics such as sex, race, age, or FVC(49-51). Differences in patient baseline FVC values may have contributed to any changes from baseline observed in this study. To account for this, we reported the relative changes observed in the imaging measurements.

Participants treated with bexotegrast in this study had lower FVCpp and longer disease duration than other bexotegrast-treated Phase 2 participants(21). Due to the small participant sample size, disease characteristics were not completely balanced. One bexotegrast-treated participant also had COVID-19 and low adherence to the study drug (65% adherence) during the treatment period, both of which may have confounded results as worsening interstitial lung disease and reduced pulmonary perfusion have been described in some patients after COVID-19(25, 52).

In conclusion, ^{68}Ga-CBP8 PET detected antifibrotic effects and potential favorable lung remodeling with bexotegrast. This study used a complementary approach to evaluate the effect of bexotegrast on both lung structure and function using multimodal PET and DCE-MRI. This approach detected improvements in quantifiable structural changes that may lead to clinically meaningful effects in patients with IPF. Treatment with bexotegrast improved FVC, cough severity, and prognostic biomarkers, suggesting its potential for disease modification. Late-stage evaluation of bexotegrast is currently underway in the enrolling BEACON-IPF study (NCT06097260).

Acknowledgments

The authors thank the clinical site staff and patients who participated in this study.

AJRCCM Articles in Press. Published March 28, 2025 as 10.1164/rccm.202410-1934OC

Data sharing statement

Clinical trial registration number: NCT05621252.

Pliant Therapeutics, Inc., ("Pliant") understands and acknowledges the need to share clinical study data with the research community in an open and transparent manner. In furtherance of its research efforts, a member of the scientific community may request aggregated deidentified clinical data collected during a clinical study after its public disclosure by Pliant and filing of any related intellectual property protection. To the extent that Pliant has any additional supporting documentation or summary data, it may, at its discretion, also make such information available. Pliant will take into consideration any reasonable request that it receives pertaining to clinical data that have been accepted and published by a journal. Prior to receipt of clinical study data, Pliant and the requesting institution shall enter into an agreement that takes into consideration applicable data privacy laws and the use of the clinical study data for research purposes only. All requests for access to clinical study data must be submitted in writing to scientificcommunications@pliantrx.com.

Role of the study sponor

This study was sponsored by Pliant Therapeutics, Inc. The study sponsor was involved in the study design, data analysis, and preparation of the manuscript.

Author disclosures

AJRCCM Articles in Press. Published March 28, 2025 as 10.1164/rccm.202410-1934OC

SB Montesi served on the advisory committee for APIE Therapeutics and Pliant Therapeutics, Inc.; served as a consultant for DevPro, Gilead, Pieris, Roche, Accendatech USA, and Mediar Therapeutics; served in a leadership role for Massachusetts Pulmonary Society; received research support from American Thoracic Society, Boehringer Ingelheim, Merck, National Scleroderma Foundation, National Institutes of Health/National Heart, Lung, and Blood Institute, Pliant Therapeutics, Inc., Three Lakes Foundation, and United Therapeutics; received royalties from UpToDate; served as speaker for Cowen; and received travel support from DevPro and Pliant Therapeutics. **GP Cosgrove, A Clark, M Decaris, CN Barnes,** and **ÉA Lefebvre** were employees of Pliant Therapeutics, Inc., at the time of this analysis. **SM Turner** is a former employee of Pliant Therapeutics, Inc. **IY Zhou** received research support from Reveal Pharmaceuticals. **N Efthimiou, A Susnjar, C Catana,** and **C Fromson** have no competing interests. **P Caravan** has equity in Collagen Medical LLC and Reveal Pharmaceuticals; has consulting income from Collagen Medical LLC and Reveal Pharmaceuticals; and received research support from Transcode Therapeutics and Pliant Therapeutics, Inc.

AJRCCM Articles in Press. Published March 28, 2025 as 10.1164/rccm.202410-1934OC

References

1. Lederer DJ, Martinez FJ. Idiopathic Pulmonary Fibrosis. N Engl J Med. 2018;379(8):797-8.

2. Raghu G, Collard HR, Egan JJ, Martinez FJ, Behr J, Brown KK, et al. An official ATS/ERS/JRS/ALAT statement: idiopathic pulmonary fibrosis: evidence-based guidelines for diagnosis and management. Am J Respir Crit Care Med. 2011;183(6):788-824.

3. Khalil W, Xia H, Bodempudi V, Kahm J, Hergert P, Smith K, et al. Pathologic Regulation of Collagen I by an Aberrant Protein Phosphatase 2A/Histone Deacetylase C4/MicroRNA-29 Signal Axis in Idiopathic Pulmonary Fibrosis Fibroblasts. Am J Respir Cell Mol Biol. 2015;53(3):391-9.

4. Murtha LA, Schuliga MJ, Mabotuwana NS, Hardy SA, Waters DW, Burgess JK, et al. The Processes and Mechanisms of Cardiac and Pulmonary Fibrosis. Front Physiol. 2017;8:777.

5. Kuhn C, 3rd, Boldt J, King TE, Jr., Crouch E, Vartio T, McDonald JA. An immunohistochemical study of architectural remodeling and connective tissue synthesis in pulmonary fibrosis. Am Rev Respir Dis. 1989;140(6):1693-703. doi: 10.1164/ajrccm/140.6.1693. PubMed PMID: 2604297.

6. Marinkovic A, Liu F, Tschumperlin DJ. Matrices of physiologic stiffness potently inactivate idiopathic pulmonary fibrosis fibroblasts. Am J Respir Cell Mol Biol. 2013;48(4):422-30.

AJRCCM Articles in Press. Published March 28, 2025 as 10.1164/rccm.202410-1934OC

7. Zhou Y, Huang X, Hecker L, Kurundkar D, Kurundkar A, Liu H, et al. Inhibition of mechanosensitive signaling in myofibroblasts ameliorates experimental pulmonary fibrosis. J Clin Invest. 2013;123(3):1096-108.

8. Ley B, Bradford WZ, Vittinghoff E, Weycker D, du Bois RM, Collard HR. Predictors of Mortality Poorly Predict Common Measures of Disease Progression in Idiopathic Pulmonary Fibrosis. Am J Respir Crit Care Med. 2016;194(6):711-8.

9. Kärkkäinen M, Kettunen HP, Nurmi H, Selander T, Purokivi M, Kaarteenaho R. Comparison of disease progression subgroups in idiopathic pulmonary fibrosis. BMC Pulm Med. 2019;19(1):228.

10. Sesé L, Nunes H, Cottin V, Israel-Biet D, Crestani B, Guillot-Dudoret S, et al. Gender Differences in Idiopathic Pulmonary Fibrosis: Are Men and Women Equal? Front Med (Lausanne). 2021;8:713698.

11. Mai TH, Han LW, Hsu JC, Kamath N, Pan L. Idiopathic pulmonary fibrosis therapy development: a clinical pharmacology perspective. Ther Adv Respir Dis. 2023;17:17534666231181537.

12. Rozenberg D, Sitzer N, Porter S, Weiss A, Colman R, Reid WD, et al. Idiopathic Pulmonary Fibrosis: A Review of Disease, Pharmacological, and Nonpharmacological Strategies With a Focus on Symptoms, Function, and Health-Related Quality of Life. J Pain Symptom Manage. 2020;59(6):1362-78.

13. Shi N, Wang Z, Zhu H, Liu W, Zhao M, Jiang X, et al. Research progress on drugs targeting the TGF-beta signaling pathway in fibrotic diseases. Immunol Res. 2022;70(3):276-88.

AJRCCM Articles in Press. Published March 28, 2025 as 10.1164/rccm.202410-1934OC

14. Aschner Y, Downey GP. Transforming Growth Factor-beta: Master Regulator of the Respiratory System in Health and Disease. Am J Respir Cell Mol Biol. 2016;54(5):647-55.

15. Frangogiannis N. Transforming growth factor-beta in tissue fibrosis. J Exp Med. 2020;217(3):e20190103.

16. Saito A, Horie M, Nagase T. TGF-beta Signaling in Lung Health and Disease. Int J Mol Sci. 2018;19(8):2460.

17. Saini G, Porte J, Weinreb PH, Violette SM, Wallace WA, McKeever TM, et al. alphavbeta6 integrin may be a potential prognostic biomarker in interstitial lung disease. Eur Respir J. 2015;46(2):486-94.

18. Horan GS, Wood S, Ona V, Li DJ, Lukashev ME, Weinreb PH, et al. Partial inhibition of integrin alpha(v)beta6 prevents pulmonary fibrosis without exacerbating inflammation. Am J Respir Crit Care Med. 2008;177(1):56-65.

19. Decaris ML, Schaub JR, Chen C, Cha J, Lee GG, Rexhepaj M, et al. Dual inhibition of alpha(v)beta(6) and alpha(v)beta(1) reduces fibrogenesis in lung tissue explants from patients with IPF. Respir Res. 2021;22(1):265.

20. Diebold RJ, Eis MJ, Yin M, Ormsby I, Boivin GP, Darrow BJ, et al. Early-onset multifocal inflammation in the transforming growth factor beta 1-null mouse is lymphocyte mediated. Proc Natl Acad Sci U S A. 1995;92(26):12215-9.

21. Lancaster L, Cottin V, Ramaswamy M, Wuyts WA, Jenkins RG, Scholand MB, et al. Bexotegrast in Patients with Idiopathic Pulmonary Fibrosis: The INTEGRIS-IPF Study. Am J Respir Crit Care Med. 2024;210(4):424-34.

AJRCCM Articles in Press. Published March 28, 2025 as 10.1164/rccm.202410-1934OC

22. Montesi SB, Izquierdo-Garcia D, Desogere P, Abston E, Liang LL, Digumarthy S, et al. Type I Collagen-targeted Positron Emission Tomography Imaging in Idiopathic Pulmonary Fibrosis: First-in-Human Studies. Am J Respir Crit Care Med. 2019;200(2):258-61.

23. Desogere P, Tapias LF, Hariri LP, Rotile NJ, Rietz TA, Probst CK, et al. Type I collagen-targeted PET probe for pulmonary fibrosis detection and staging in preclinical models. Sci Transl Med. 2017;9(384):eaaf4696.

24. Moon BF, Zhou IY, Ning Y, Chen YI, Le Fur M, Shuvaev S, et al. Simultaneous Positron Emission Tomography and Molecular Magnetic Resonance Imaging of Cardiopulmonary Fibrosis in a Mouse Model of Left Ventricular Dysfunction. J Am Heart Assoc. 2024;13(14):e034363.

25. Zhou IY, Mascia M, Alba GA, Magaletta M, Ginns LC, Caravan P, et al. Dynamic Contrast-enhanced MRI Demonstrates Pulmonary Microvascular Abnormalities Months After SARS-CoV-2 Infection. Am J Respir Crit Care Med. 2023;207(12):1636-9.

26. Zhang WJ, Niven RM, Young SS, Liu YZ, Parker GJ, Naish JH. T1-weighted Dynamic Contrast-enhanced MR Imaging of the Lung in Asthma: Semiquantitative Analysis for the Assessment of Contrast Agent Kinetic Characteristics. Radiology. 2016;278(3):906-16.

27. Amundsen T, Torheim G, Waage A, Bjermer L, Steen PA, Haraldseth O. Perfusion magnetic resonance imaging of the lung: characterization of pneumonia and chronic obstructive pulmonary disease. A feasibility study. J Magn Reson Imaging. 2000;12(2):224-31.

AJRCCM Articles in Press. Published March 28, 2025 as 10.1164/rccm.202410-1934OC

28. Montesi SB, Zhou IY, Liang LL, Digumarthy SR, Mercaldo S, Mercaldo N, et al. Dynamic contrast-enhanced magnetic resonance imaging of the lung reveals important pathobiology in idiopathic pulmonary fibrosis. ERJ Open Res. 2021;7(4):00907-2020.

29. Montesi SB, Cosgrove GP, Turner S, Zhou I, Efthimiou N, Susnjar A, et al. Bexotegrast reduces type 1 collagen deposition in participants with idiopathic pulmonary fibrosis (IPF) after 12 weeks of therapy. Eur Respir J. 2024;64(suppl 68):OA1058.

30. Raghu G, Remy-Jardin M, Myers JL, Richeldi L, Ryerson CJ, Lederer DJ, et al. Diagnosis of Idiopathic Pulmonary Fibrosis. An Official ATS/ERS/JRS/ALAT Clinical Practice Guideline. Am J Respir Crit Care Med. 2018;198(5):e44-e68.

31. Montesi SB. 2020 American Thoracic Society BEAR Cage Winning Proposal: Collagen-targeted Positron Emission Tomography Imaging as a Novel Biomarker of Treatment Response in Idiopathic Pulmonary Fibrosis. Am J Respir Crit Care Med. 2021;203(9):1065-7.

32. Ambrosini V, Zompatori M, De Luca F, Antonia D, Allegri V, Nanni C, et al. 68Ga-DOTANOC PET/CT allows somatostatin receptor imaging in idiopathic pulmonary fibrosis: preliminary results. J Nucl Med. 2010;51(12):1950-5.

33. Win T, Thomas BA, Lambrou T, Hutton BF, Screaton NJ, Porter JC, et al. Areas of normal pulmonary parenchyma on HRCT exhibit increased FDG PET signal in IPF patients. Eur J Nucl Med Mol Imaging. 2014;41(2):337-42.

34. Kim GHJ, Goldin JG, Hayes W, Oh A, Soule B, Du S. The value of imaging and clinical outcomes in a phase II clinical trial of a lysophosphatidic acid receptor antagonist in idiopathic pulmonary fibrosis. Ther Adv Respir Dis. 2021;15:17534666211004238.

AJRCCM Articles in Press. Published March 28, 2025 as 10.1164/rccm.202410-1934OC

35. Lancaster L, Goldin J, Trampisch M, Kim GH, Ilowite J, Homik L, et al. Effects of Nintedanib on Quantitative Lung Fibrosis Score in Idiopathic Pulmonary Fibrosis. Open Respir Med J. 2020;14:22-31.

36. Cuenod CA, Balvay D. Perfusion and vascular permeability: basic concepts and measurement in DCE-CT and DCE-MRI. Diagn Interv Imaging. 2013;94(12):1187-204.

37. Weatherley ND, Eaden JA, Hughes PJC, Austin M, Smith L, Bray J, et al. Quantification of pulmonary perfusion in idiopathic pulmonary fibrosis with first pass dynamic contrast-enhanced perfusion MRI. Thorax. 2021;76(2):144-51.

38. Thannickal VJ, Henke CA, Horowitz JC, Noble PW, Roman J, Sime PJ, et al. Matrix biology of idiopathic pulmonary fibrosis: a workshop report of the national heart, lung, and blood institute. Am J Pathol. 2014;184(6):1643-51.

39. Nakamori S, Dohi K, Ishida M, Goto Y, Imanaka-Yoshida K, Omori T, et al. Native T1 Mapping and Extracellular Volume Mapping for the Assessment of Diffuse Myocardial Fibrosis in Dilated Cardiomyopathy. JACC Cardiovasc Imaging. 2018;11(1):48-59.

40. Luetkens JA, Klein S, Träber F, Schmeel FC, Sprinkart AM, Kuetting DLR, et al. Quantification of Liver Fibrosis at T1 and T2 Mapping with Extracellular Volume Fraction MRI: Preclinical Results. Radiology. 2018;288(3):748-54.

41. Podolsky MJ, Yang CD, Valenzuela CL, Datta R, Huang SK, Nishimura SL, et al. Age-dependent regulation of cell-mediated collagen turnover. JCI Insight. 2020;5(10):e137519.

42. Ryerson CJ, Abbritti M, Ley B, Elicker BM, Jones KD, Collard HR. Cough predicts prognosis in idiopathic pulmonary fibrosis. Respirology. 2011;16(6):969-75.

AJRCCM Articles in Press. Published March 28, 2025 as 10.1164/rccm.202410-1934OC

43. Bargagli E, Di Masi M, Perruzza M, Vietri L, Bergantini L, Torricelli E, et al. The pathogenetic mechanisms of cough in idiopathic pulmonary fibrosis. Intern Emerg Med. 2019;14(1):39-43.

44. Xie S, Macedo P, Hew M, Nassenstein C, Lee KY, Chung KF. Expression of transforming growth factor-beta (TGF-beta) in chronic idiopathic cough. Respir Res. 2009;10(1):40.

45. Martin Nguyen A, Bacci ED, Vernon M, Birring SS, Rosa C, Muccino D, et al. Validation of a visual analog scale for assessing cough severity in patients with chronic cough. Ther Adv Respir Dis. 2021;15:17534666211049743.

46. Organ LA, Duggan AR, Oballa E, Taggart SC, Simpson JK, Kang'ombe AR, et al. Biomarkers of collagen synthesis predict progression in the PROFILE idiopathic pulmonary fibrosis cohort. Respir Res. 2019;20(1):148.

47. Bowman WS, Newton CA, Linderholm AL, Neely ML, Pugashetti JV, Kaul B, et al. Proteomic biomarkers of progressive fibrosing interstitial lung disease: a multicentre cohort analysis. Lancet Respir Med. 2022;10(6):593-602.

48. Tatler AL, Goodwin AT, Gbolahan O, Saini G, Porte J, John AE, et al. Amplification of TGFbeta Induced ITGB6 Gene Transcription May Promote Pulmonary Fibrosis. PLoS One. 2016;11(8):e0158047.

49. Kolb M, Flaherty KR, Silva RS, Prasse A, Vancheri C, Mueller H, et al. Effect of Nintedanib in Patients with Progressive Pulmonary Fibrosis in Subgroups with Differing Baseline Characteristics. Adv Ther. 2023;40(12):5536-46.

AJRCCM Articles in Press. Published March 28, 2025 as 10.1164/rccm.202410-1934OC

50. Costabel U, Inoue Y, Richeldi L, Collard HR, Tschoepe I, Stowasser S, et al. Efficacy of Nintedanib in Idiopathic Pulmonary Fibrosis across Prespecified Subgroups in INPULSIS. Am J Respir Crit Care Med. 2016;193(2):178-85.

51. Noble PW, Albera C, Bradford WZ, Costabel U, du Bois RM, Fagan EA, et al. Pirfenidone for idiopathic pulmonary fibrosis: analysis of pooled data from three multinational phase 3 trials. Eur Respir J. 2016;47(1):243-53.

52. Gallay L, Uzunhan Y, Borie R, Lazor R, Rigaud P, Marchand-Adam S, et al. Risk Factors for Mortality after COVID-19 in Patients with Preexisting Interstitial Lung Disease. Am J Respir Crit Care Med. 2021;203(2):245-9.

AJRCCM Articles in Press. Published March 28, 2025 as 10.1164/rccm.202410-1934OC

Figure Legends

Figure 1. Overview of (**A**) Study Design and (**B**) Participant Disposition.

Figure 2. (**A**) Representative PET Images of Total Lung Collagen at Baseline and Week 12 and (**B**) Absolute and (**C**) Individual Change From Baseline in Top Quartile SUV of Whole Lung at Week 12.

PET, positron emission tomography; SUV, standardized uptake value. The length of the box represents the range between the 25th and 75th percentiles, the whiskers represent the maximum and minimum, and the horizontal line in the box represents the median. All individual data points are displayed. The nonadherent/COVID-19 participant in the bexotegrast group is indicated by red circle. Baseline FVC and FVCpp values for representative bexotegrast and placebo images were 2400 mL and 66% and 1700 mL and 49%, respectively.

Figure 3. Absolute Change From Baseline in the Top Quartile SUV of (**A**) Collective Subpleural and Central Regions of the Lung and (**B**) Individual Lung Regions.

SUV, standardized uptake value. The values for lower subpleural, middle subpleural, upper subpleural, lower central, middle central, and upper central are the average of the left and right values for each region. The length of the box represents the range between the 25th and 75th percentiles, the whiskers represent the maximum and minimum, and the horizontal line in the box represents the median. All individual data

AJRCCM Articles in Press. Published March 28, 2025 as 10.1164/rccm.202410-1934OC

points are displayed. The nonadherent/COVID-19 participant in the bexotegrast group is indicated by red circle.

Figure 4. (**A**) Absolute and (**B**) Individual Change From Baseline in Peak Enhancement and (**C**) Absolute and (**D**) Individual Change From Baseline in $k_{washout}$ in Whole Lung at Week 12. (**E**) Representative Parametric Maps of Peak Enhancement and $k_{washout}$ at Baseline and Week 12.

The length of the box represents the range between the 25th and 75th percentiles, the whiskers represent the maximum and minimum, and the horizontal line in the box represents the median. All individual data points are displayed. The nonadherent/COVID-19 participant in the bexotegrast group is indicated by red circle. Baseline FVC and FVCpp values for the representative bexotegrast and placebo images were 4500 mL and 92% and 2640 mL and 69%, respectively.

Figure 5. LS Mean (SE) Change From Baseline in (**A**) FVC (**B**) FVCpp and (**C**) Mean (SE) Change From Baseline in Cough Severity at Week 12.
*One placebo-treated participant did not have acceptable quality spirometry post baseline. FVC, forced vital capacity; FVCpp, percent predicted forced vital capacity; LS, least squares; VAS, visual analog scale.

Figure 6. LS Mean (SE) Change From Baseline in (**A**) PRO-C3 and (**B**) ITGB6 at Week 12.

AJRCCM Articles in Press. Published March 28, 2025 as 10.1164/rccm.202410-1934OC

ITGB6, integrin beta-6; LS, least squares; PRO-C3, type III collagen synthesis neoepitope.

AJRCCM Articles in Press. Published March 28, 2025 as 10.1164/rccm.202410-1934OC

Table 1. Baseline Demographics and Disease Characteristics (Safety Population)

Characteristic	**Bexotegrast 160 mg (n=7)**	**Placebo (n=3)**
Age, mean (SD), years	69.1 (8.3)	74.0 (2.0)
Male, n (%)	6 (85.7)	3 (100)
Race, n (%)		
White	6 (85.7)	3 (100)
Asian	1 (14.3)	0
BMI, mean (SD), kg/m^2	26.9 (3.9)	26.9 (3.2)
Time since IPF diagnosis, median (IQR), months	50.0 (22.0-70.0)	9.0 (7.0-72.0)
Standard of care use, n (%)	6 (85.7)	2 (66.7)
Nintedanib	5 (71.4)	1 (33.3)
Pirfenidone	1 (14.3)	1 (33.3)
FVC		
Median (IQR), mL	2750.0 (2400.0-3080.0)	2410.0 (1700.0-2640.0)
Percent predicted, median (IQR)	66.0 (56.0-92.0)	58.0 (49.0-69.0)
Cough severity, median (IQR), mm	28.0 (5.0-66.0)	19.0 (0.0-45.0)

AJRCCM Articles in Press. Published March 28, 2025 as 10.1164/rccm.202410-1934OC

GAP stage, n (%)		
I	4 (57.1)	0
II	2 (28.6)	2 (66.7)
III	1 (14.3)	1 (33.3)
^{68}Ga-CBP8 top quartile SUV, mean (SD)		
Whole lung	0.888 (0.138)	0.977 (0.142)
Subpleural	1.123 (0.208)	1.193 (0.150)
Central	0.709 (0.112)	0.817 (0.071)

BMI, body mass index; FVC, forced vital capacity; GAP, gender-age-physiology; IPF, idiopathic pulmonary fibrosis.

AJRCCM Articles in Press. Published March 28, 2025 as 10.1164/rccm.202410-1934OC

Table 2. Nature and Frequency of TEAEs Over 12 Weeks of Treatment (Safety Population)

TEAE, n (%) of participants	**Bexotegrast 160 mg (n=7)**	**Placebo (n=3)**
TEAE	6 (85.7)	1 (33.3)
TEAE related to study drug	5 (71.4)	1 (33.3)
Serious TEAE	0	0
Grade ≥3 TEAE	1 (14.3)*	0
Grade ≥3 TEAE related to study drug	1 (14.3)*	0
TEAE leading to interruption of study drug	1 (14.3)†	0
TEAE leading to withdrawal of study drug	0	0
TEAE leading to early termination from study	0	0
TEAE leading to death	0	0
Most frequent TEAEs (n>1)		
Cough	4 (57.1)‡	0
Diarrhea	3 (42.9)§	1 (33.3)

TEAE, treatment-emergent adverse event.

*Participant experienced Grade 3 TEAEs of increased amylase and increased lipase.

†Participant with COVID-19.

AJRCCM Articles in Press. Published March 28, 2025 as 10.1164/rccm.202410-1934OC

‡All cough events occurred post Week 12 (end of treatment) during the 14-day follow-up period.

§All events of diarrhea were considered mild. The 3 participants were taking nintedanib, which was listed as an alternative cause.

AJRCCM Articles in Press. Published March 28, 2025 as 10.1164/rccm.202410-1934OC

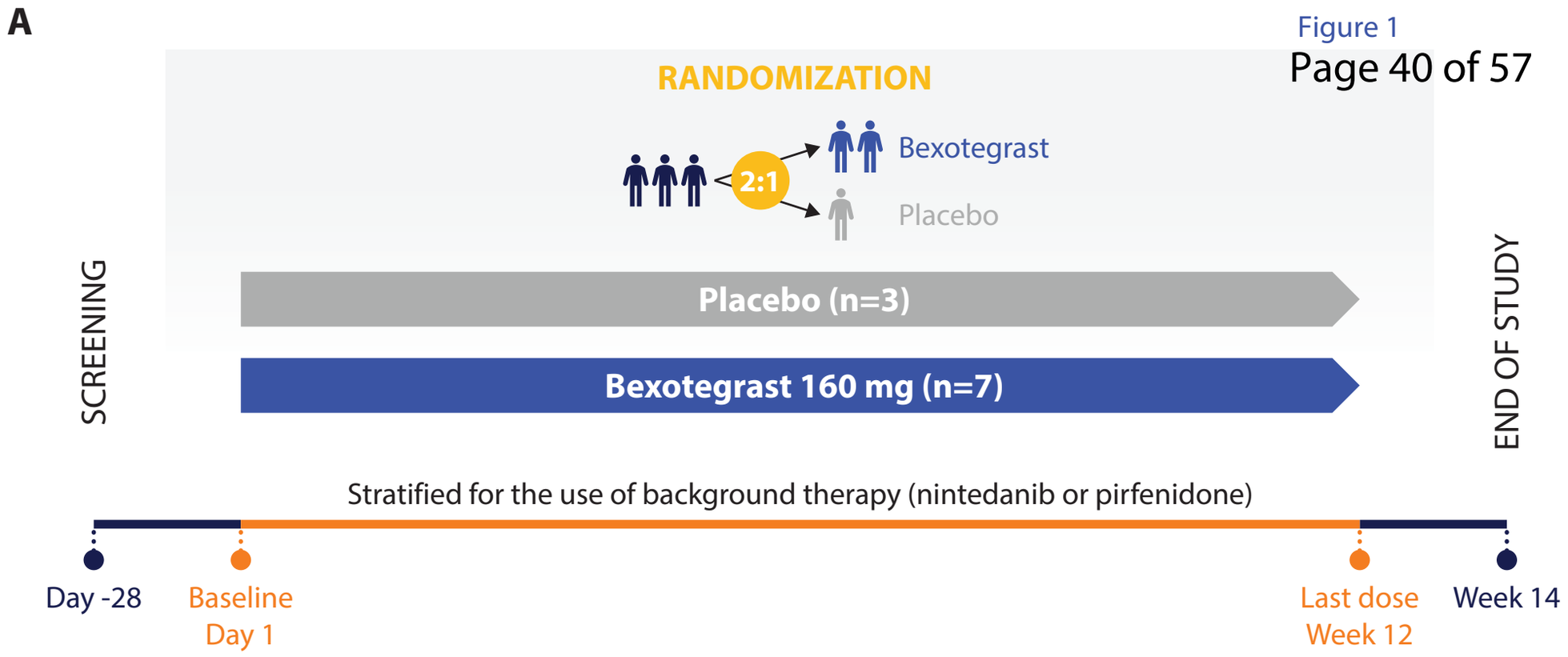

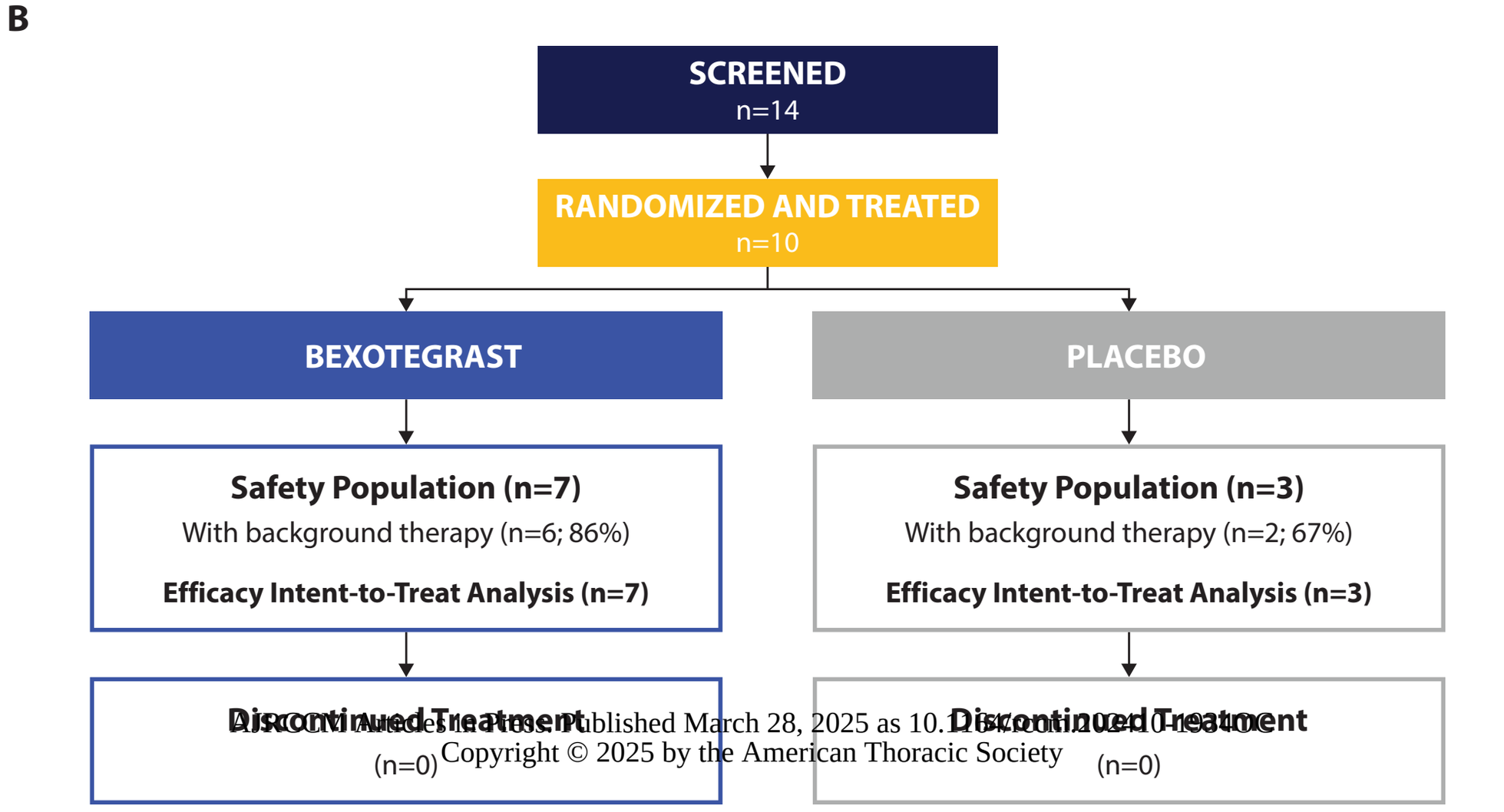

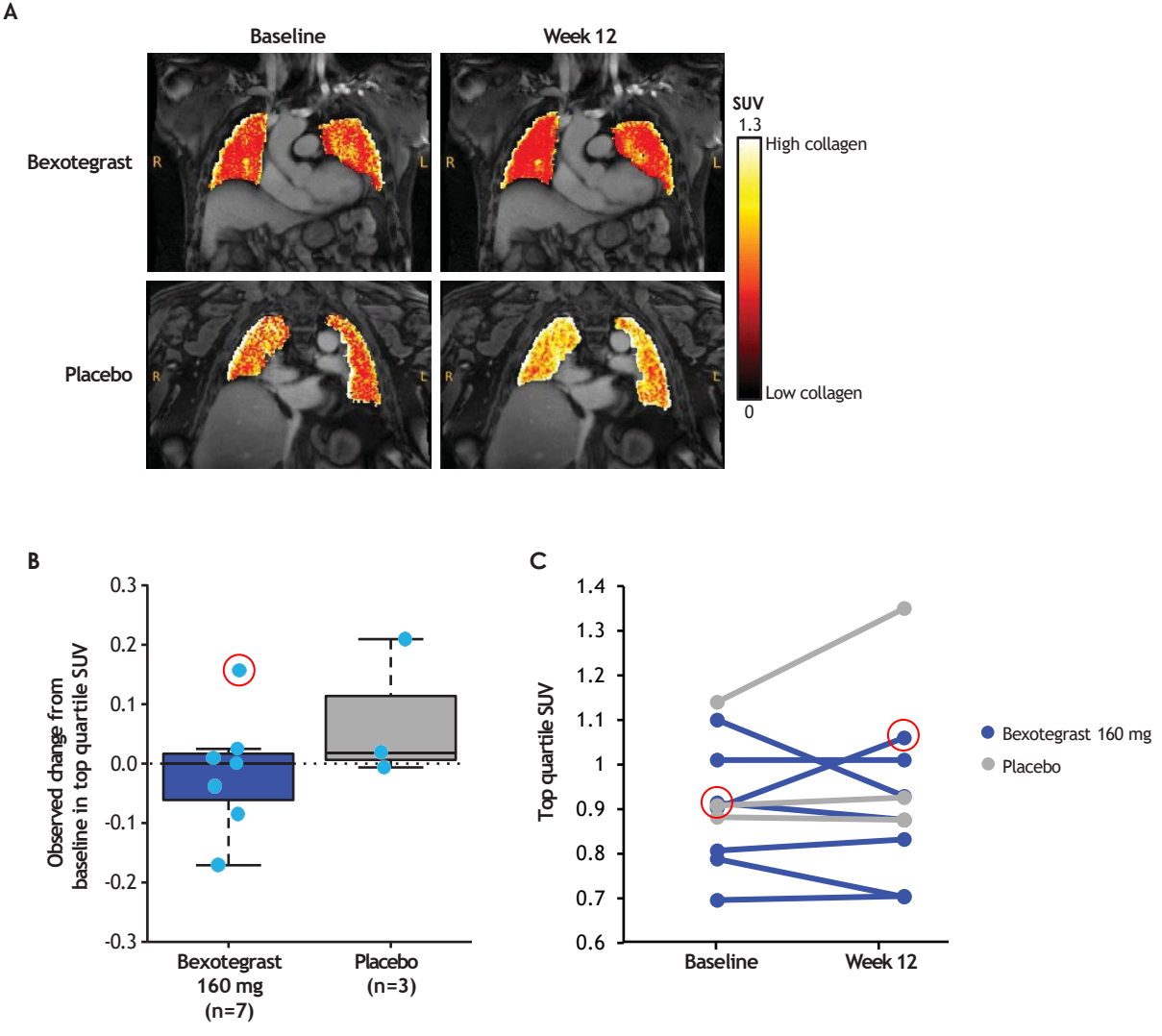

AJRCCM Articles in Press. Published March 28, 2025 as 10.1164/rccm.202410-1934OC

Figure 2

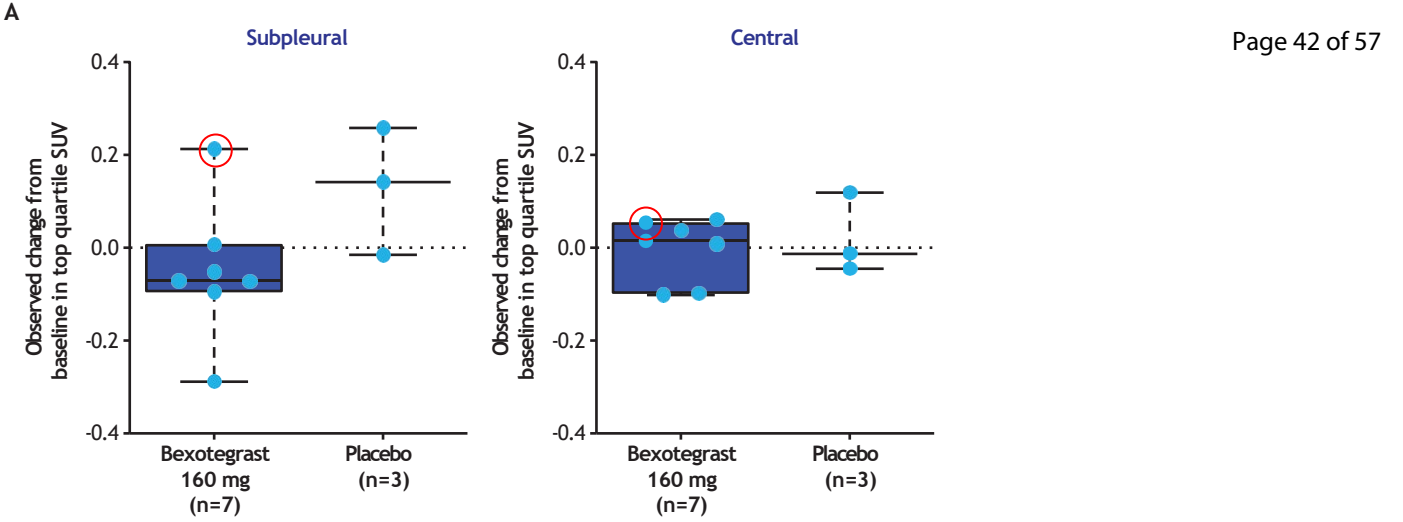

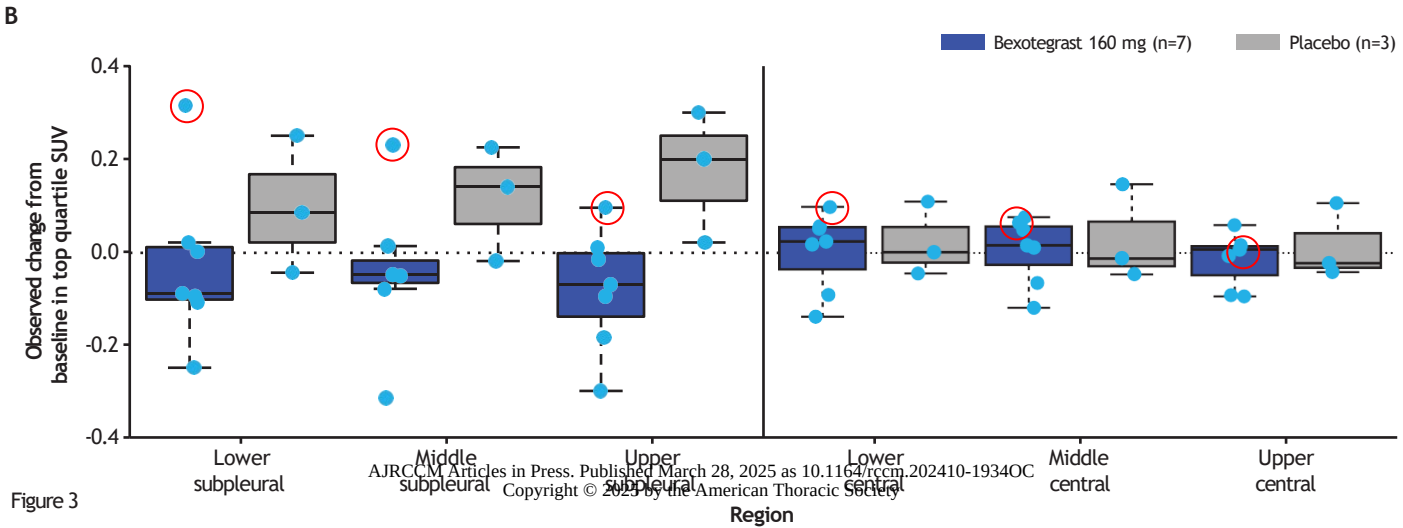

Figure 3

AJRCCM Articles in Press. Published March 28, 2025 as 10.1164/rccm.202410-1934OC

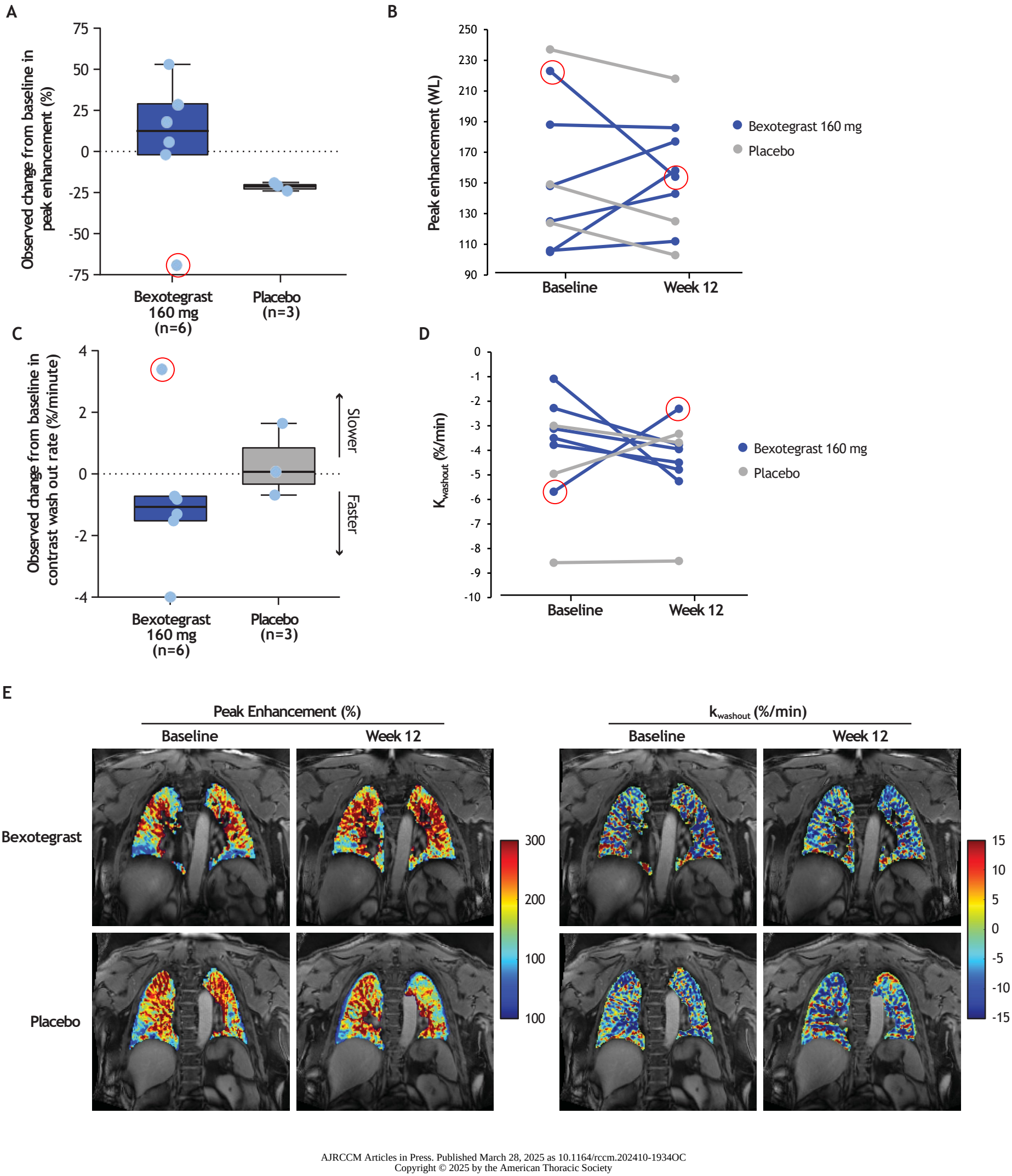

Figure 4

AJRCCM Articles in Press. Published March 28, 2025 as 10.1164/rccm.202410-1934OC

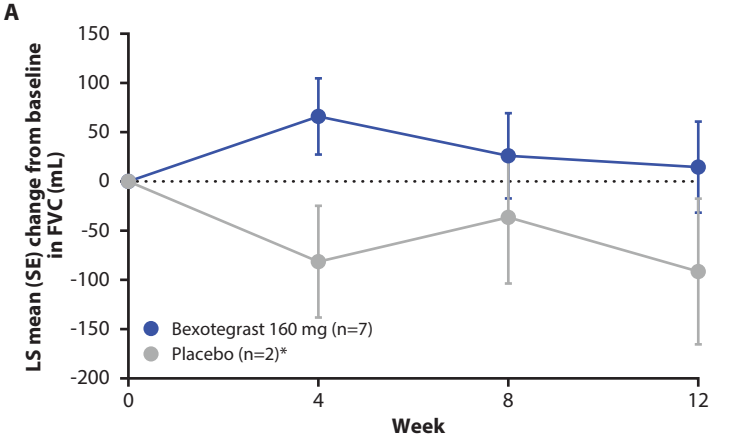

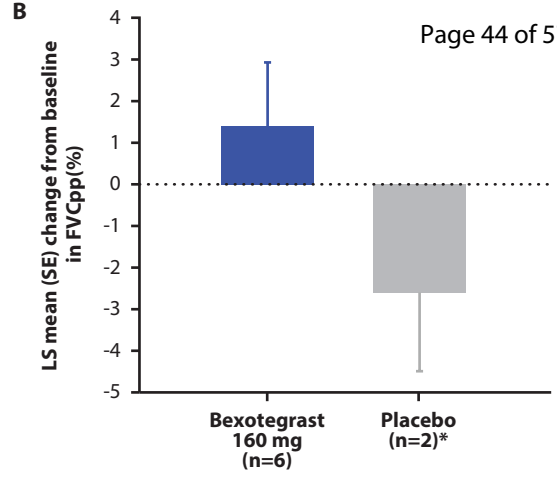

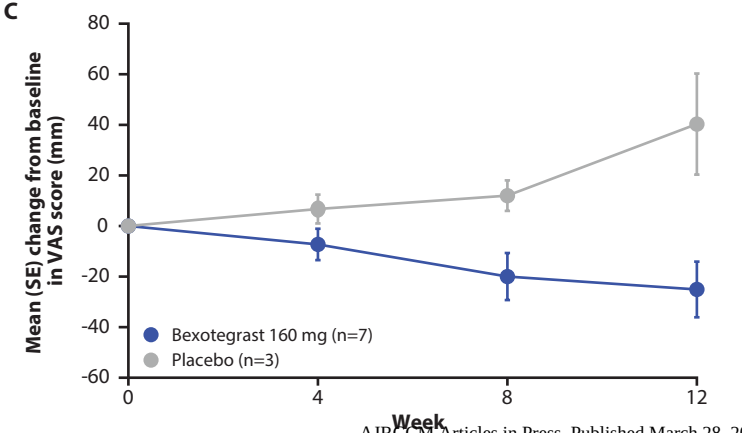

AJRCCM Articles in Press. Published March 28, 2025 as 10.1164/rccm.202410-1934OC

Figure 5

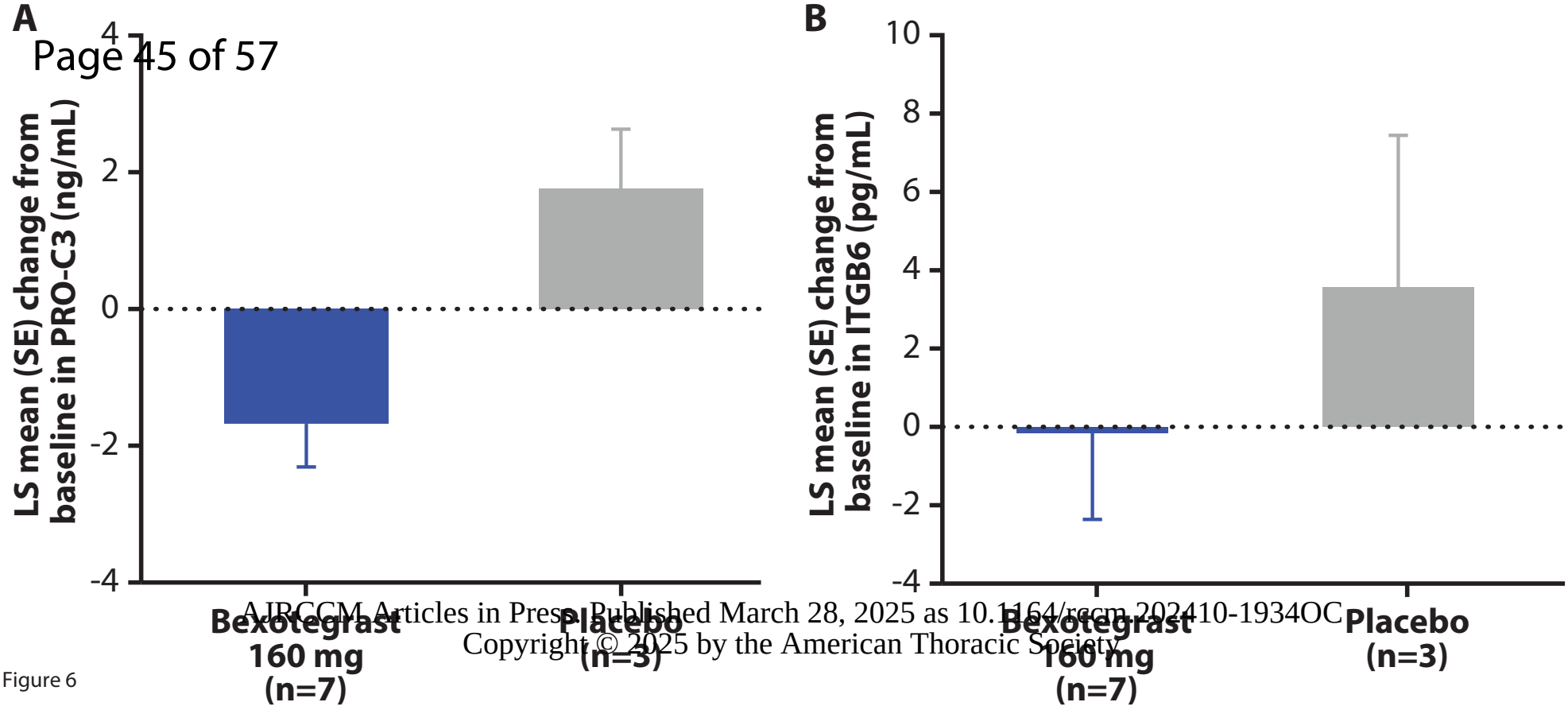

AJRCCM Articles in Press. Published March 28, 2025 as 10.1164/rccm.202410-1934OC

Figure 6

Dual $\alpha_v\beta_6$ and $\alpha_v\beta_1$ Inhibition Over 12 Weeks Reduces Active Type 1 Collagen Deposition in Individuals with Idiopathic Pulmonary Fibrosis: A Phase 2, Double-Blind, Placebo-controlled Clinical Trial

Sydney B. Montesi, Gregory P. Cosgrove, Scott M. Turner, Iris Y. Zhou, Nikos Efthimiou, Antonia Susnjar, Ciprian Catana, Caroline Fromson, Annie Clark, Martin Decaris, Chris N. Barnes, Éric A. Lefebvre, Peter Caravan

ONLINE DATA SUPPLEMENT

AJRCCM Articles in Press. Published March 28, 2025 as 10.1164/rccm.202410-1934OC

Supplemental Methods

Procedures

^{68}Ga-CBP8 positron emission tomography (PET) and magnetic resonance imaging (MRI) of the thorax were performed simultaneously on a Siemens Biograph mMR scanner (Siemens Healthineers, Erlangen, Germany). All PET was performed after intravenous injection of the collagen-targeted probe, ^{68}Ga-CBP8, at a mean (range) radiochemical dose of 197 MBq (125-295 MBq) per administration. The average PET start time was 44 minutes post-injection, with an average acquisition time of 35 minutes. The PET data were reconstructed in a 2.1 × 2.1 × 2.0 mm^3 voxel size using the ordered subset expectation maximization algorithm with 21 subsets and 3 iterations. All corrections, per the manufacturer's settings, were applied. The images were filtered post-reconstruction with a 2 × 2 × 2 mm^3 Gaussian filter. The MRI-based attenuation correction maps were manually corrected for any artifacts.

A 3D whole-lung region of interest (ROI) was defined over the lung parenchyma across all imaging slices, excluding the heart, pulmonary artery, descending aorta, large hilar vessels, and large airways. The whole-lung ROI was divided into 12 regional ROIs by segmenting each lung (left and right) into 3 parts with equal lengths along the axial direction (upper, middle, and lower). Additionally, each lung was divided into subpleural (outer 1.6 cm of the lung) and central regions, similar to prior studies (1). Summary standardized uptake value (SUV) metrics for each region included mean SUV, the mean of all SUVs within a region, maximum SUV, single maximum SUV within a region, top quartile SUV, and the mean of the top 25% SUVs within a region.

AJRCCM Articles in Press. Published March 28, 2025 as 10.1164/rccm.202410-1934OC

DCE-MRI was performed using a radial sampling sequence: 15° flip angle, 1.0-ms echo time, 3.4-ms repetition time, field of view of 410 × 410 mm^2, voxel size of 2.1 × 2.1 × 2.5 mm^3, and 72 slices. Serial volumetric pulmonary images were acquired during free breathing and reconstructed to a temporal resolution of 2.75 seconds (2). Imaging acquisition started 60 seconds prior to the injection of gadoterate meglumine 0.05 mmol/kg (Guerbet, Villepinte, France) at a rate of 4 mL/s and continued for 360 seconds after the start of contrast injection. Due to technical problems, DCE-MRI data was not available for 1 participant. The same 3D whole-lung ROI used for PET analysis was used for DCE-MRI analysis. The dynamic curve of the ROI was calculated as the percentage of signal intensity change over baseline, where baseline signal intensity was calculated by averaging the dynamic acquisitions before the bolus of contrast arrived in the pulmonary artery. Parameters of interest were extracted from the dynamic curve of the ROI, including peak enhancement, the maximum percentage of relative signal intensity change over baseline, and late-phase washout slope ($k_{washout}$), calculated by linear fitting of the points between 60 seconds post-injection and the last acquisition.

For other exploratory endpoints, FVC was assessed by spirometry at Baseline and Weeks 4, 8, and 12. Cough severity was assessed by patient-reported visual analog scale at Baseline and Weeks 2, 4, 8, and 12. Plasma and serum biomarkers were collected at Baseline, Week 4, and Week 12.

Statistical analysis

A sample size of approximately 12 participants (8 receiving bexotegrast 160 mg, 4 receiving placebo) was expected to provide a meaningful evaluation of the safety,

AJRCCM Articles in Press. Published March 28, 2025 as 10.1164/rccm.202410-1934OC

tolerability, and pharmacodynamics of bexotegrast in participants with IPF. Two analysis populations were included: a safety population (all randomized participants who received ≥1 dose of study drug) and a pharmacodynamic population (all randomized participants who received the study drug and had results from baseline and the post-baseline PET/MRI scan).

Given the small sample size anticipated in this study, all comparisons are descriptive and focus primarily on change from baseline. While several summary metrics have been used for SUVs (eg, mean and maximum) (3,4), this study used the top quartile SUV, which is the mean SUV for the highest 25% of SUVs within a region. The top quartile was identified as a relevant measurement for detecting active disease given the heterogeneity of fibrosis in each lung region; the mean SUV could be attenuated by areas that lack fibrosis, and the maximum may only apply to a very small region within the lung. Values for subpleural whole lung and central whole lung were calculated by averaging SUV summary metrics across both lungs and individual regions (upper, middle, and lower regions) as applicable.

For forced vital capacity (FVC), a repeated-measures mixed model was used to assess the difference between treatment groups with respect to change from baseline to Weeks 4, 8, and 12. Fixed effects in the model were treatment group, visit, treatment-by-visit interaction term, background therapy status (pirfenidone or nintedanib; yes or no), and baseline FVC. An unstructured covariance was used as the within-participant covariance structure. Separate models were conducted for absolute FVC and forced vital capacity percent predicted (FVCpp) analyses.

AJRCCM Articles in Press. Published March 28, 2025 as 10.1164/rccm.202410-1934OC

References

1. Montesi SB, Izquierdo-Garcia D, Desogere P, Abston E, Liang LL, Digumarthy S, et al. Type I Collagen-targeted Positron Emission Tomography Imaging in Idiopathic Pulmonary Fibrosis: First-in-Human Studies. Am J Respir Crit Care Med. 2019;200(2):258-61.
2. Montesi SB, Zhou IY, Liang LL, Digumarthy SR, Mercaldo S, Mercaldo N, et al. Dynamic contrast-enhanced magnetic resonance imaging of the lung reveals important pathobiology in idiopathic pulmonary fibrosis. ERJ Open Res. 2021;7(4):00907-2020.
3. Liao X, Liu M, Li S, Huang W, Guo C, Liu J, et al. The value on SUV-derived parameters assessed on (18)F-FDG PET/CT for predicting mediastinal lymph node metastasis in non-small cell lung cancer. BMC Med Imaging. 2023;23(1):49.
4. Wehlte L, Walter J, Daisenberger L, Kuhnle F, Ingenerf M, Schmid-Tannwald C, et al. The Association between the Body Mass Index, Chronic Obstructive Pulmonary Disease and SUV of the Non-Tumorous Lung in the Pretreatment [(18)F]FDG-PET/CT of Patients with Lung Cancer. Diagnostics (Basel). 2024;14(11):1139.

AJRCCM Articles in Press. Published March 28, 2025 as 10.1164/rccm.202410-1934OC

Supplemental Figures

Figure E1. Individual Observed Percent Change From Baseline in the Top Quartile SUV of (A) Whole Lung and (B) Subpleural and Central Lung Regions*

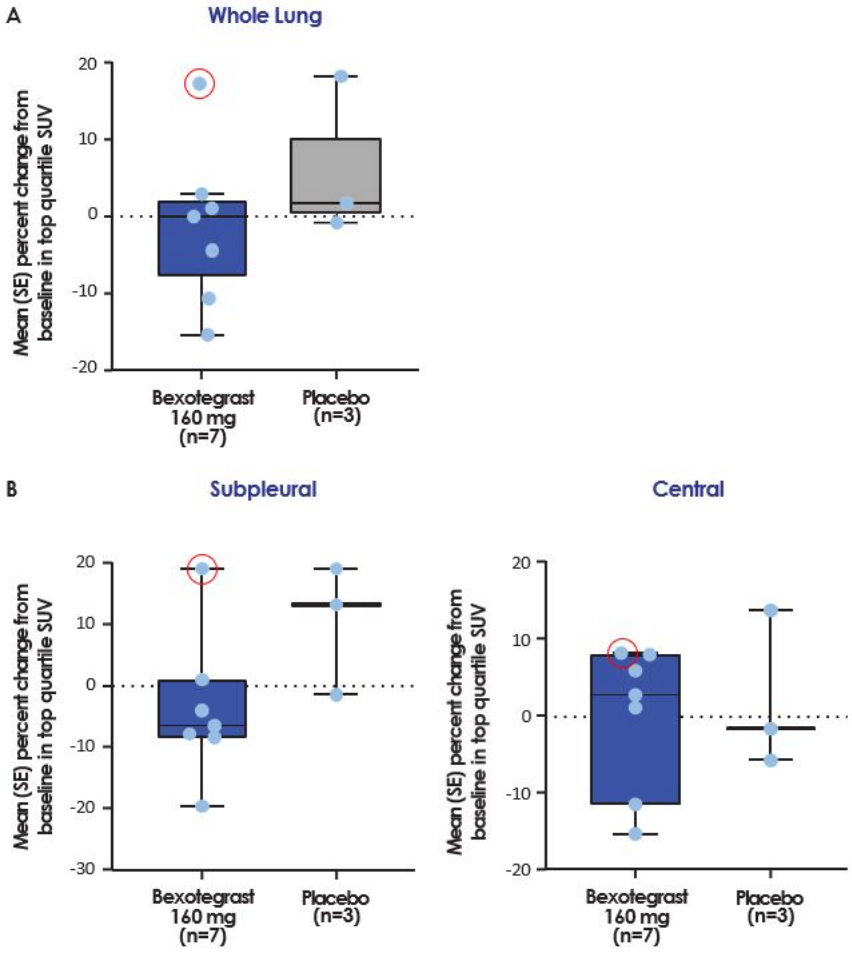

SUV, standardized uptake value. *The values for lower subpleural, middle subpleural, upper subpleural, lower central, middle central, and upper central are the average of the left and right values for each region. The length of the box represents the range between the 25th and 75th percentiles, the whiskers represent the maximum and minimum, and the horizontal line in the box represents the median. All individual data points are displayed. Change was of smaller magnitude in the central region than in

AJRCCM Articles in Press. Published March 28, 2025 as 10.1164/rccm.202410-1934OC

subpleural regions. The nonadherent/COVID-19 participant in the bexotegrast group is indicated by red circle.

AJRCCM Articles in Press. Published March 28, 2025 as 10.1164/rccm.202410-1934OC

Figure E2: Individual Change From Baseline in (**A**) FVC*, (**B**) FVCpp*, and (**C**) Cough Severity at Week 12

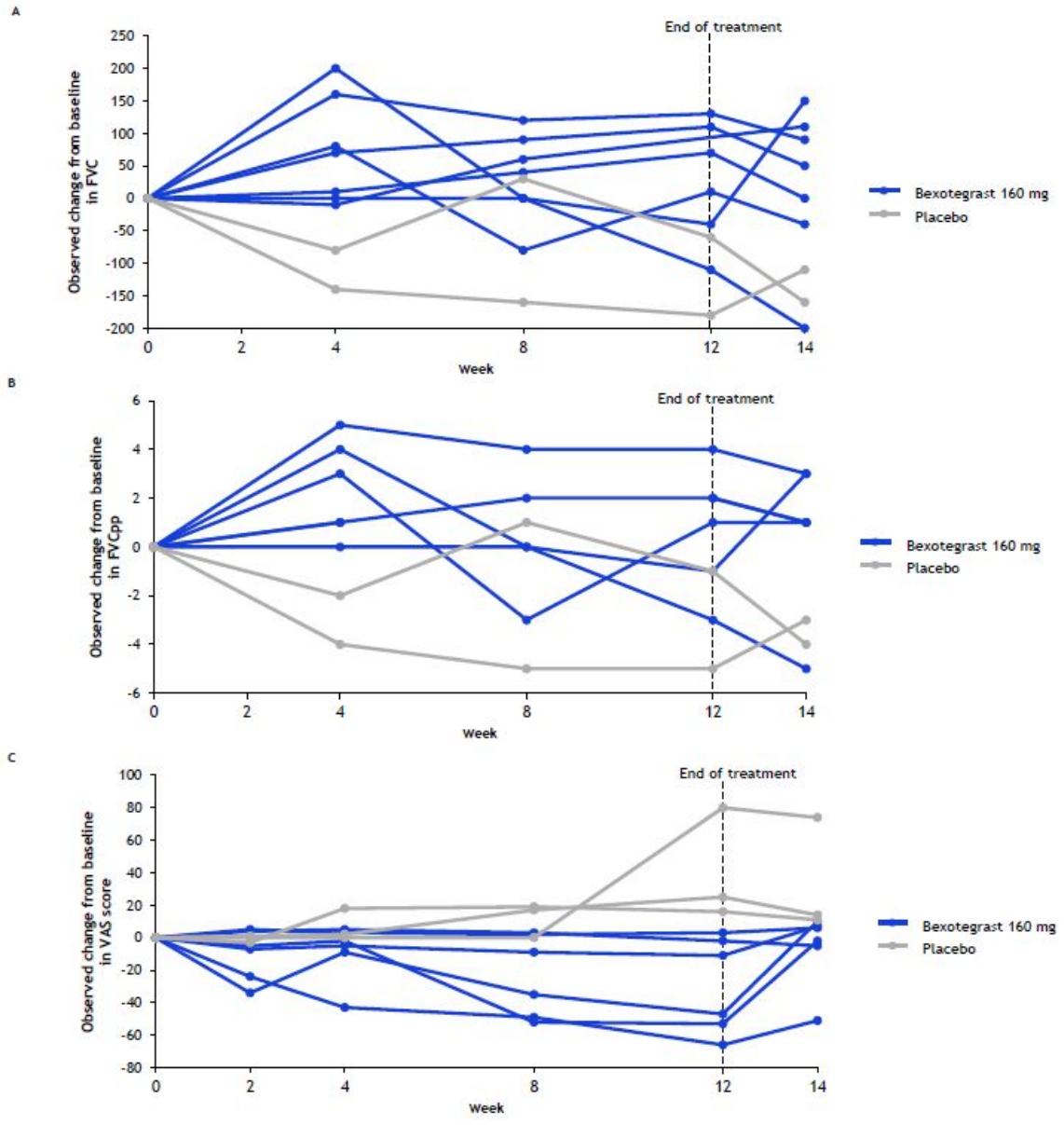

*One placebo-treated participant did not have acceptable quality spirometry post baseline.

FVC, forced vital capacity; FVCpp, percent predicted forced vital capacity VAS, visual analog scale.

AJRCCM Articles in Press. Published March 28, 2025 as 10.1164/rccm.202410-1934OC

Figure E3: Individual Change From Baseline in (**A**) PRO-C3 and (**B**) ITGB6 at Week 12

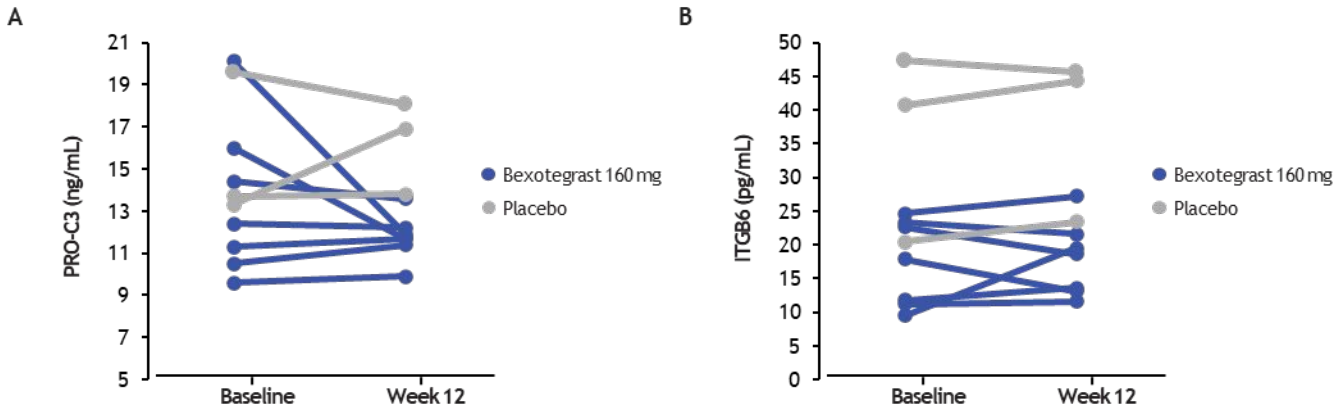

ITGB6, integrin beta-6; PRO-C3, type III collagen synthesis neoepitope.

The nonadherent/COVID-19 participant in the bexotegrast group is indicated by red circle.

AJRCCM Articles in Press. Published March 28, 2025 as 10.1164/rccm.202410-1934OC

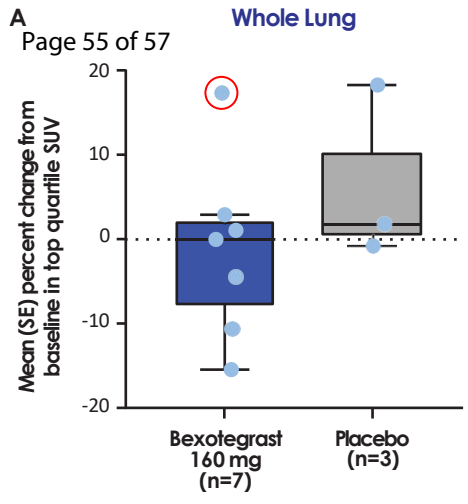

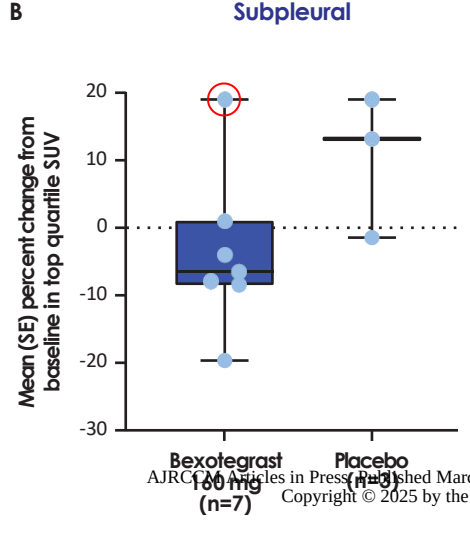

A

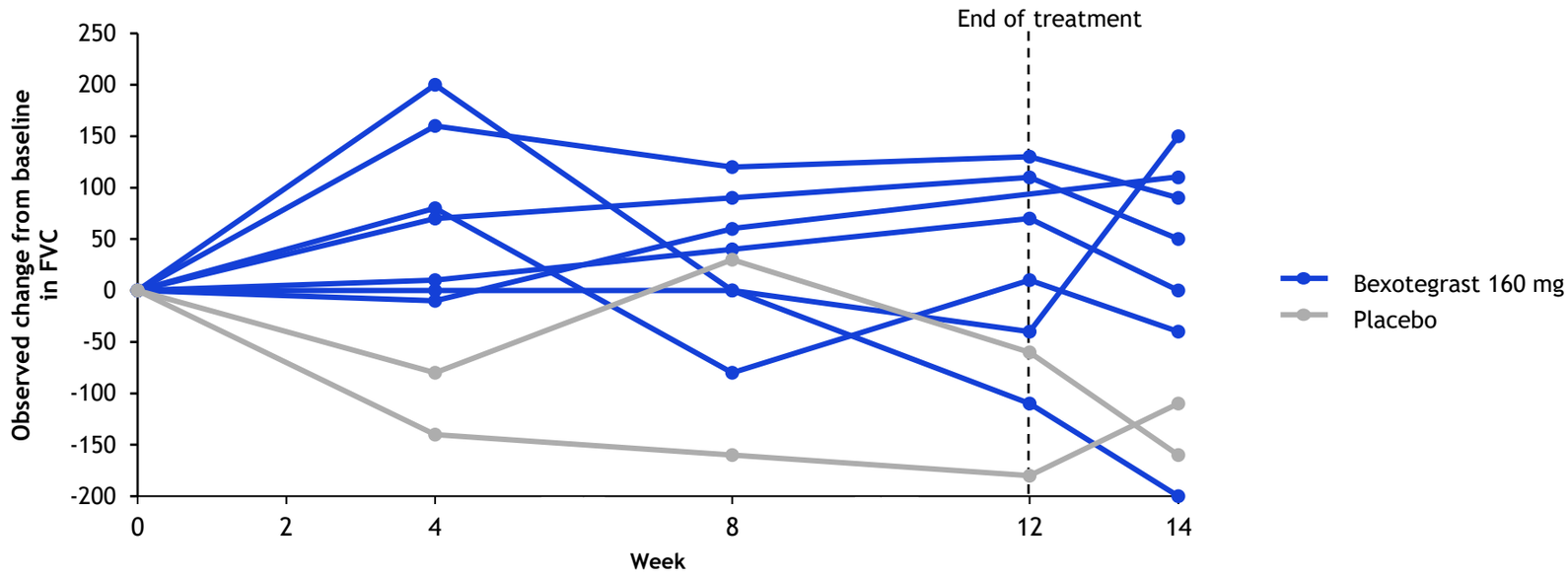

B

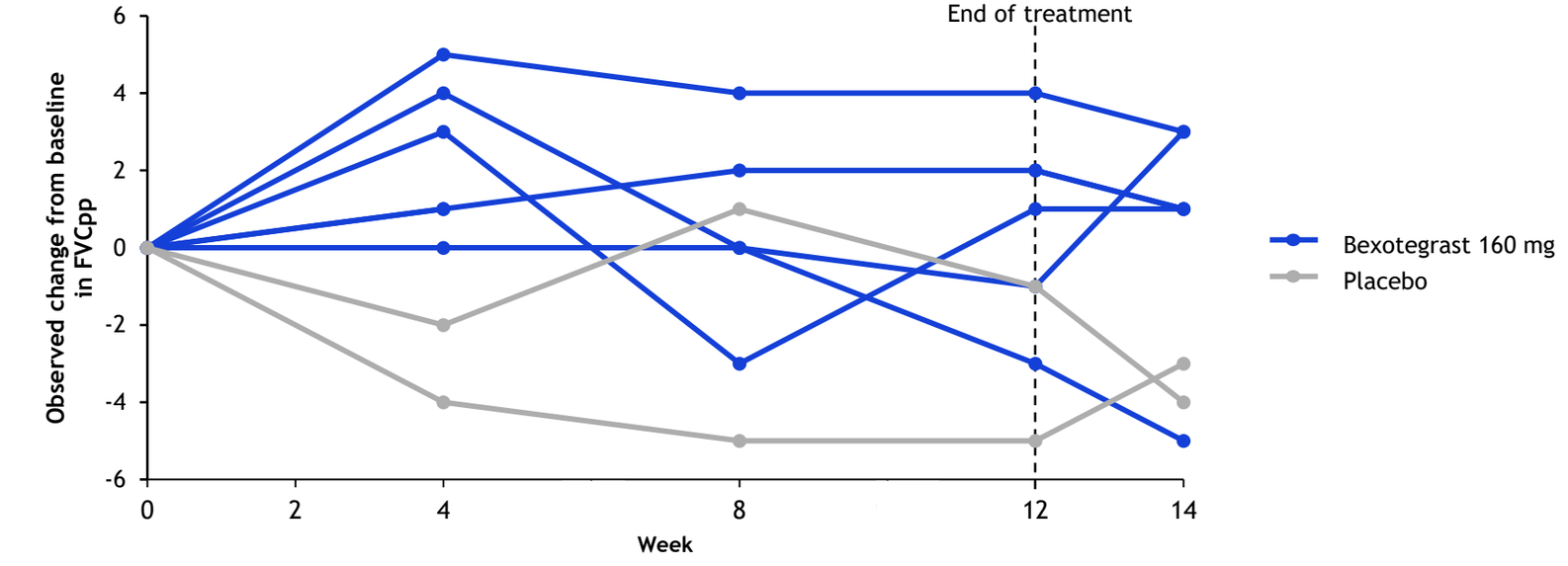

C

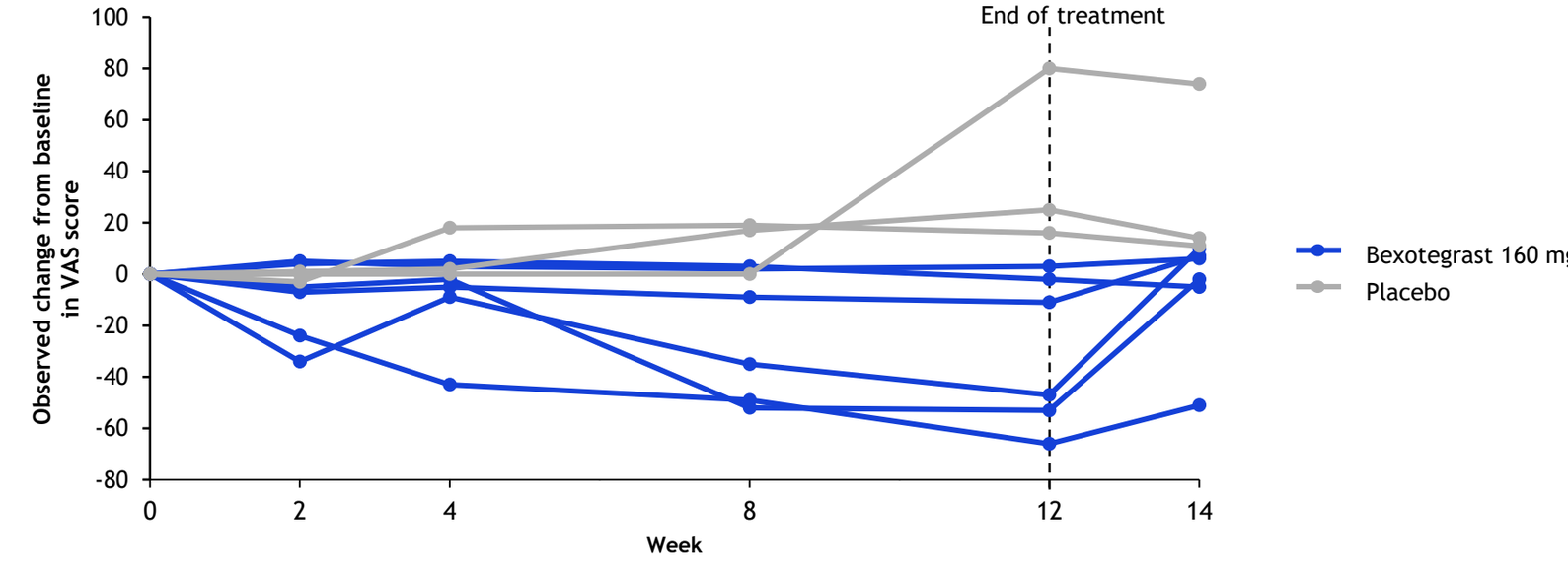

AJRCCM Articles in Press. Published March 28, 2025 as 10.1164/rccm.202410-1934OC

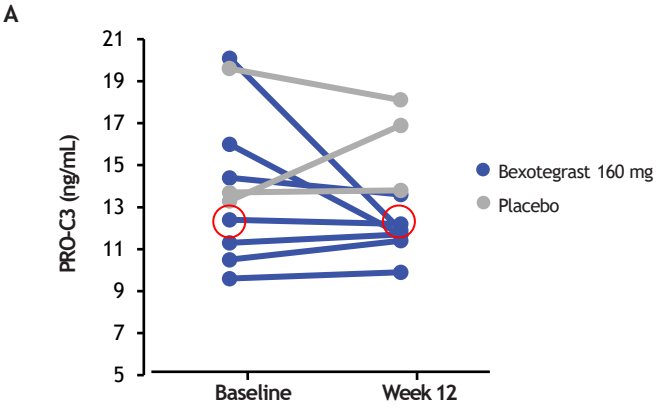

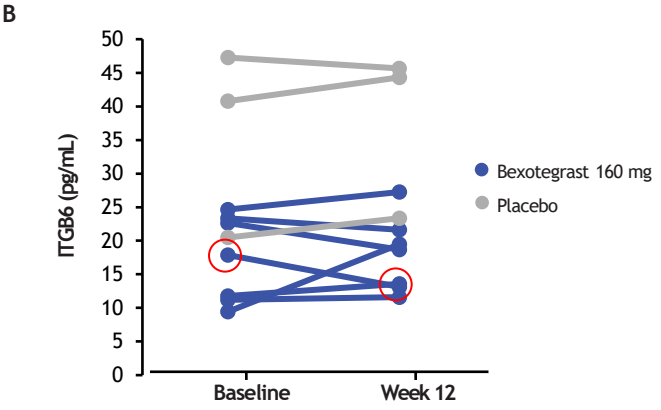

AJRCCM Articles in Press. Published March 28, 2025 as 10.1164/rccm.202410-1934OC